Electronic Supplementary Material (ESI) for Organic Chemistry Frontiers.

Supporting Information

Xanthrysols A−D, Novel Meroterpenoids with Antiviral Activities from *Xanthostemon chrysanthus*†

Fen Liu,‡[a, c] Ji-Hong Gu,‡[b] Zi-Yue Zhang[a], Qiong Zhan[a], Hai-Xia Yang[a], Yun Hu[a], Jin-Yan Zhang[a], Wei Tang*[a], Wen-Cai Ye,*[a] and Lei Wang*[a]

[a]State Key Laboratory of Bioactive Molecules and Druggability Assessment, Center for Bioactive Natural Molecules and Innovative Drugs Research, College of Pharmacy, Jinan University, and Center for Natural Bioactive Molecules and Innovative Drugs, College of Pharmacy, Jinan University, Guangzhou 510632, P. R. China.

[b]Science and Technology Innovation Center, Guangzhou University of Chinese Medicine, Guangzhou 510405, P. R. China.

[c]Key Laboratory of Medicinal Resources Chemistry and Pharmacology in Wuling Mountainous of Hunan Province College, Jishou University, Jishou 416000, P. R. China.

---

*Corresponding authors. Tel./fax: + 86 20 85223553.

E-mail addresses: cpuwanglei@126.com (L. Wang), chywc@aliyun.com (W.-C. Ye), tangw@jnu.edu.cn (W. Tang).

Table of Contents

1 General experimental procedures

Melting points were obtained on an X-5 micro melting point apparatus without correction (Fukai Instrument, Beijing, China). Optical rotations were measured on a JASCO P-2000 digital polarimeter (Jasco, Tokyo, Japan). UV spectra were recorded on a JASCO V-550 UV−vis spectrophotometer (Jasco, Tokyo, Japan). IR spectra were determined on a JASCO FT/IR-4600 plus Fourier transform infrared spectrometer (Jasco, Tokyo, Japan) using KBr pellets. ECD spectra were obtained on a Chirascan Plus qCD spectropolarimeter (Applied Photophysics Limited, Leatherhead, UK). HR-ESI-MS were obtained on an Agilent 6210 ESI-TOF mass spectrometer (Agilent Technologies, CA, USA). NMR spectra were measured on a Bruker AV-500 spectrometer (Bruker, Fällanden, Switzerland). Single-crystal data were performed using an Agilent Gemini S Ultra diffractometer and Cu Kα radiation (λ = 1.54178 Å). Column chromatography (CC) was carried out on a silica gel (200−300 mesh, Qingdao Marine Chemical Inc., Qingdao, China), ODS (Merck, Darmstadt, Germany), or Sephadex LH-20 (Pharmacia Biotec AB, Uppsala, Sweden). Preparative HPLC was performed on an Agilent system equipped with a semipreparative column (Phenomenex C18, 10 × 250 mm^2). The chiral separation was carried out using Phenomenex Lux Cellulose-1 and Industries ChromegaChiral CC4 (250 × 4.6 mm, 5 μm) (4.6 × 250 mm^2) chiral HPLC columns. All solvents used in CC and HPLC were of analytical (Shanghai Chemical Plant, Shanghai, China)

2 Plant materials

The leaves of *X. chrysanthus* were collected in Guangzhou city of P. R. China in October of 2016 and identified by Prof. Guang-Xiong Zhou (Jinan University). A voucher specimen (No. 2016100501) has been deposited in the Center for Bioactive Natural Molecules and Innovative Drugs Research, Jinan University, Guangzhou, P. R. China.

3 Extraction and isolation

The air-dried leaves of *X. chrysanthus* (20 kg) were powdered and extracted with 95% EtOH for 4 times at room temperature. The crude extract (3.0 kg) was suspended in H_2O and extracted with petroleum ether (PE). The PE extract (930 g) was subjected to a silica gel CC eluted with a gradient mixture of PE/EtOAc (100:0 → 0:100) to afford

ten fractions (Fr.1–10). Fr.2 (45 g) was separated on Sephadex LH-20 (6 × 160 cm, CH_3OH/CH_2Cl_2, 1:1) to yield four fractions (Fr.2A–2D). Fr.2B (32 g) was subjected to ODS column chromatography using CH_3OH/H_2O (60:40→ 100:0) as eluent to yield Fr.2B.1−Fr.2B.40. Fr.2B.30 was separated on Sephadex LH-20 (1 × 100 cm, CH_3OH) and further purified by reversed-phase HPLC (CH_3CN/H_2O, 85:15, 3 mL/min) to afford compound **1** (12.0 mg, t_R = 16 min). Fr.3 (40 g) was separated on Sephadex LH-20 (6 × 160 cm, CH_3OH) to yield four fractions (Fr.3A–3D). Fr.3B–3D (35 g) was subjected to ODS column chromatography using CH_3OH/H_2O (60:40 → 100:0) as eluent to yield Fr.3B.1−Fr.3B.60. Fr.3B.20 was separated on Sephadex LH-20 (1 × 100 cm, CH_3OH) and further purified by reversed-phase HPLC (CH_3CN/H_2O, 75:25, 3 mL/min) to afford compounds **2** (50.2 mg, t_R = 12 min), **3** (20.5 mg, t_R = 14 min), and **4** (11.2 mg, t_R = 11 min). Fr.9 (60.7 g) was repeatedly chromatographed using silica gel CC to yield nine subfractions (Fr.9A−9I). Fr.9D (10.2 g) was subjected to ODS column chromatography using CH_3OH/H_2O (40:60 → 100:0) as an eluent to yield Fr.9D.1−Fr.9D.40. Fr.9D.5 was further purified by semipreparative HPLC (CH_3CN/H_2O, 60:40, 3 mL/min) to afford compounds **5** (20 mg) and **6** (100 mg).

Xanthrysol A (1). Yellowish oil (CH_3OH); (+)-**1** $[\alpha]_D^{26}$ + 58.9 (*c* 0.9, CH_3OH), ECD (CH_3CN) λ_{max} ($\Delta\varepsilon$) 212 (−67.7), 248 (+14.3), 284 (+30.2), 368 (+4.0); (–)-**1** $[\alpha]_D^{26}$ –58.7 (*c* 0.8, CH_3OH), ECD (CH_3CN) λ_{max} ($\Delta\varepsilon$) 212 (+67.7), 248 (−14.3), 284 (−30.2), 368 (−4.0); UV (CH_3OH) λ_{max} (log ε) 207 (3.40), 290 (3.07) nm; IR (KBr) ν_{max} 3453, 2927, 1726, 1628, 1435, 1308, 1121, 969, 697, 504 cm^{-1}; HR-ESI-MS *m/z* 535.2694 $[M+H]^+$ (calcd for $C_{32}H_{39}O_7$, 535.2690).

Xanthrysol B (2). Yellowish oil (CH_3OH); (+)-**2** $[\alpha]_D^{26}$ + 62.9 (*c* 1.0, CH_3OH), ECD (CH_3CN) λ_{max} ($\Delta\varepsilon$) 201 (+21.8), 218 (−7.2), 238 (−3.3), 285(+3.2), 373 (+1.4); (–)-**2** $[\alpha]_D^{26}$ –70.5 (*c* 1.0, CH_3OH), ECD (CH_3CN) λ_{max} ($\Delta\varepsilon$) 203 (−22.8), 218 (+6.6), 238 (+2.8), 285(−4.1), 373 (−2.1); UV (CH_3OH) λ_{max} (log ε) 207 (4.38), 291 (3.83), 369 (3.09) nm; IR (KBr) ν_{max} 3127, 2940, 1682, 1444, 1385, 1211, 1141, 844, 803, 725, 699, 601, 557, 519, 475, 431 cm^{-1}; HR-ESI-MS *m/z* 537.2844 $[M+H]^+$ (calcd for $C_{32}H_{41}O_7$, 537.2847).

Xanthrysol C (3). Yellowish blocks (CH_3OH);); m.p. 110~112 °C; (+)-**3** $[\alpha]_D^{26}$ + 46.7 (*c* 1.0, CH_3OH), ECD (CH_3CN) λ_{max} ($\Delta\varepsilon$) 223 (+20.1), 255 (+2.0), 291(−4.0), 348

(−0.9); (–)-**3** $[\alpha]_D^{26}$ –42.5 (*c* 1.0, CH_3OH), ECD (CH_3CN) λ_{max} ($\Delta\varepsilon$) 223 (−19.4), 255 (−2.4), 291(+3.1), 348 (+0.5); UV (CH_3OH) λ_{max} (log ε) 209 (5.51), 290 (5.03), 369 (4.34) nm; IR (KBr) ν_{max} 3419, 2930, 1698, 1628, 1430, 1379, 1250, 1142, 749, 699 cm^{-1}; HR-ESI-MS *m/z* 559.2663 $[M+Na]^+$ (calcd for $C_{32}H_{40}NaO_7$, 559.2666).

Xanthrysol D (4). Yellowish blocks (CH_3OH); m.p. 130~132 °C; (+)-**4** $[\alpha]_D^{26}$ + 56.5 (*c* 0.2, CH_3OH), ECD (CH_3CN) λ_{max} ($\Delta\varepsilon$) 220 (−7.3), 289 (+3.8), 369 (+1.9); (–)-**4** $[\alpha]_D^{26}$ –52.8 (*c* 0.2, CH_3OH), ECD (CH_3CN) λ_{max} ($\Delta\varepsilon$) 220 (+6.5), 289 (−2.6), 369 (−1.2); UV (CH_3OH) λ_{max} (log ε) 207 (4.22), 290 (3.65), 369 (2.83) nm; IR (KBr) ν_{max} 3415, 2922, 1685, 1633, 1618, 1427, 1376, 1302, 1257, 1125, 1062, 956, 742, 701 cm^{-1}; HR-ESI-MS *m/z* 557.2559 $[M+Na]^+$ (calcd for $C_{32}H_{38}NaO_7$, 557.2510).

Myrigalone G (5). Amorphous powder (CH_3OH); HR-ESI-MS *m/z* 287.1272 $[M + H]^+$ (calcd for $C_{17}H_{19}O_4$, 287.1278); ^1H NMR (400 MHz, $CDCl_3$) δ 7.28 (4H, overlapped), 7.19 (1H, m), 5.96 (1H, s), 3.82 (3H, s), 3.42 (2H, d, J = 7.6 Hz), 3.03 (2H, d, J = 7.6 Hz), 2.01 (3H, s) ppm; ^{13}C NMR (100 MHz, $CDCl_3$) δ 204.9, 161.4, 163.4, 159.8, 141.8, 128.6 (×4), 126.1, 104.7, 103.5, 91.6, 55.8, 45.9, 30.8, 7.2 ppm.

(*E*, *E*)-farnesoic acid (6). Yellowish oil (CH_3OH); HR-ESI-MS *m/z* 237.1852 $[M + H]^+$ (calcd for $C_{15}H_{25}O_2$, 237.1849); ^1H NMR (400 MHz, $CDCl_3$) δ 5.69 (1H, s), 5.08 (2H, overlapped), 2.18−2.19 (4H, overlapped), 2.18 (3H, s), 2.06 (2H, m), 1.98 (2H, m), 1.67 (3H, s), 1.60 (6H, overlapped) ppm; ^{13}C NMR (100 MHz, $CDCl_3$) δ 172.3, 163.1, 136.4, 131.6, 124.3, 122.8, 115.4, 41.3, 39.8, 26.8, 26.1, 25.8, 19.3, 17.8, 16.2 ppm.

4 X-Ray Crystallographic analyses of 3 and 4

The single crystals of **3** and **4** were obtained from CH_3OH solution by slow evaporation at room temperature. X-ray diffraction data were collected on an Agilent Gemini S Ultra diffractometer using Cu Kα radiation (λ = 1.54178 Å). The crystal structures were solved by direct methods and refined by full-matrix least squares on F_2 using the SHELXL-2015 program. The crystallographic data have been deposited with the Cambridge Crystallographic Data Centre (CCDC 2340348 for **3**, CCDC 2340233 for **4**).

Crystal data of **3**. $C_{32}H_{40}O_7$ (Formula weight = 536.64); Triclinic, space group $P\bar{1}$; *a*

= 10.1786(4) Å, b = 12.0107(3) Å, c = 13.3288(4) Å, α = 103.806(2)°; β = 108.912(3)°; γ = 101.165(3)°; V = 1430.37 (8) Å^3; T = 149.95 (13) K; Z = 2; ρ_{calc} = 1.246 g/cm^3; F(000) =576.0; A total of 23668 reflections in -12 ≤ h ≤12, -14 ≤ k ≤14, -16 ≤ l ≤16 were collected in the range 7.412 ≤ θ ≤148.308, of which 5709 unique reflections with $I > 2\sigma(I)$ were collected for the analysis. The final R indices [$I > 2\sigma(I)$]: R_1 =0.0463, wR_2 =0.1291, R indices (all data): R_1=0.0505, wR_2 =0.1333; the goodness of fit on F^2 was 1.060.

Crystal data of **4**. $C_{32}H_{38}O_7$ (Formula weight = 534.62); Triclinic, space group $P\bar{1}$; a = 9.57700(10) Å, b = 10.91970(10) Å, c = 14.0119(2) Å, α = 92.2630(10)°; β = 97.3280(10)°; γ = 102.0190(10)°; V = 1418.21(3) Å^3; T = 100.00(10) K; Z = 2; ρ_{calc} = 1.252 g/cm^3; F(000) = 572.0; A total of 50257 reflections in -11 ≤ h ≤ 11, -13 ≤ k ≤ 13, -17 ≤ l ≤ 17 were collected in the range 8.298 ≤ θ ≤ 147.382, of which 5650 unique reflections with $I > 2\sigma(I)$ were collected for the analysis. The final R indices [$I > 2\sigma(I)$]: R_1 = 0.0370, wR_2 = 0.0979, R indices (all data): R_1= 0.0383, wR_2 = 0.0990; the goodness of fit on F^2 was 1.029.

5 Antiviral effect assay

5.1 Cells, viruses, and antiviral compounds

HEp-2 (a human epithelial type 2 cell line) and Vero (an African green monkey kidney cell line) cells were purchased from the American Type Culture Collection (ATCC, USA) and cultured in Dulbecco's modified Eagle's medium (DMEM) supplemented with 10% fetal bovine serum (FBS, Biological Industries) containing 1% Penicillin-Streptomycin solution. RSV A2 and HSV-1 F strains were propagated in HEp-2 and Vero cells, respectively. Viral suspensions were stored at −80°C. Compound samples were dissolved in Dimethyl sulfoxide (DMSO) at 50 mM for subsequent experiments.

5.2 Antiviral assay

Vero and HEp-2 cells were seeded in 96-well plates and incubated overnight. The cells were treated with DMSO or diluted compounds, and then inoculated with HSV-1 and RSV, respectively. After incubation for 36 h or 60 h, the cytopathic effect (CPE) induced by the HSV-1 and RSV were determined as previously described.[1-2]

5.3 Confocal assay

HEp-2 cells were seeded in confocal dishes and inoculated with RSV in the presence of DMSO, ribavirin, or compound **1**. At 48 post-infection, the fusion (F) glycoprotein in the cells was stained with anti-RSV F and Alexa flour 488-conjugated secondary antibodies. The cell nucleus was stained with 4',6-diamidino-2-phenylindole (DAPI). After washing with PBS, the fluorescence intensity in cells was detected with a laser scanning confocal microscopy.

5.4 Time of addition assay

Vero or HEp-2 cells were infected with HSV-1/GFP and RSV respectively, and then treated with compound 1 or DMSO at indicated time points after viral infection. At 24 or 48 h post-infection, the cells were fixed with 4% paraformaldehyde in PBS and permeabilized with 0.1% Triton X-100 for 10 min. For RSV infection, the cells were incubated with RSV F specific antibody, followed by incubation with Alexa flour 488-conjugated secondary antibody. All the cells were stained with DAPI. After washing with PBS, the fluorescence in Vero or HEp-2 cells was measured using a fluorescence microscope.

6 Chiral separation of 1–4

The racemic mixtures (±)-**1**−(±)-**4** were subjected to a chiral HPLC column to afford the optical pure enantiomers (+)-**1**, (−)-**1**, (+)-**2**, (−)-**2**, (+)-**3**, (−)-**3**, (+)-**4**, and (−)-**4**.

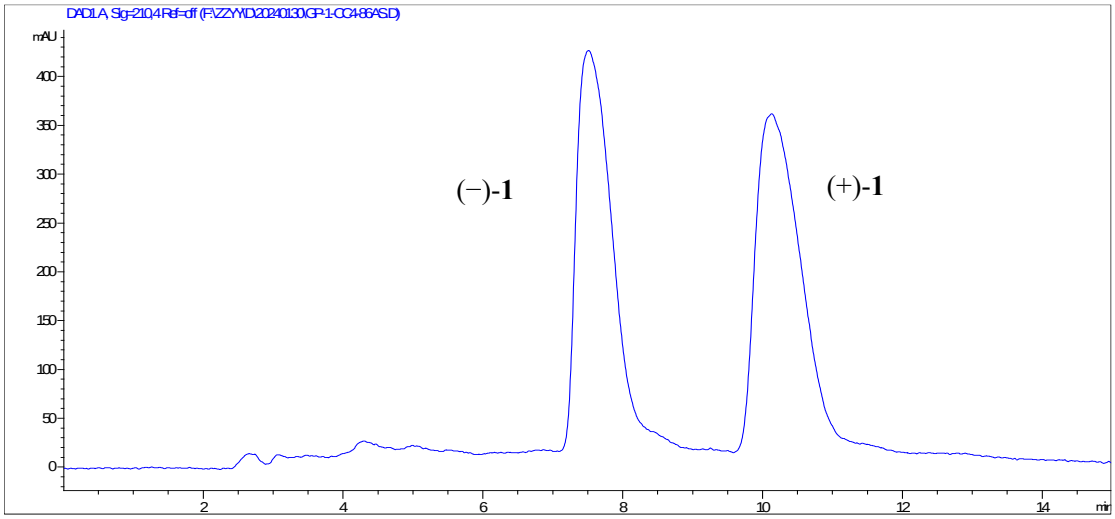

Fig. S1. Chiral HPLC Chromatogram of **1** [column: Industries ChromegaChiral CC4 (4.6 × 250 mm, 5 μm), mobile phase: $CH_3CN/H_2O/CF_3COOH$ (86:14:0.1, *V/V/V*), flow rate: 1.0 mL/min, detection wavelength: 210 nm].

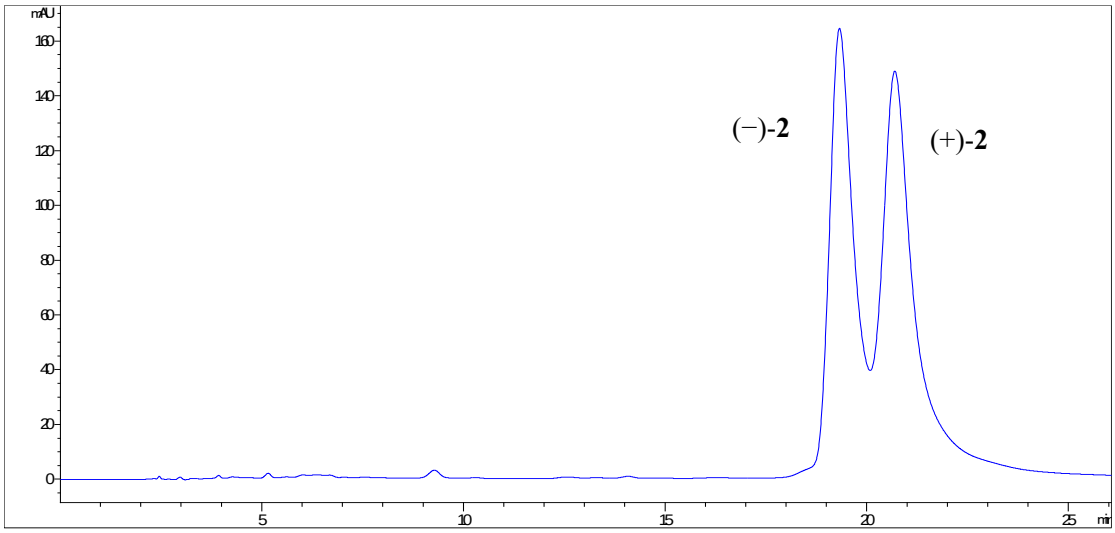

Fig. S2. Chiral HPLC Chromatogram of **2** [column: Phenomenex Cellulose-1 (4.6 × 250 mm, 5 μm), mobile phase: $CH_3CN/H_2O/CF_3COOH$ (70:30:0.1, *V/V/V*), flow rate: 1.0 mL/min, detection wavelength: 280 nm].

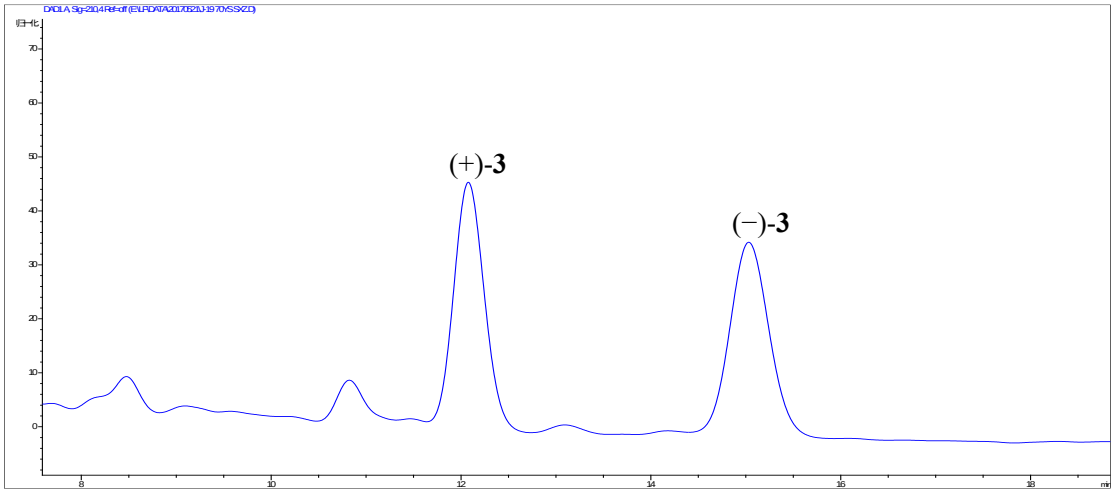

Fig. S3. Chiral HPLC Chromatogram of **3** [column: Phenomenex Cellulose-1 (4.6 × 250 mm, 5 μm), mobile phase: $CH_3CN/H_2O/CF_3COOH$ (70:30:0.1, *V/V/V*), flow rate: 1.0 mL/min, detection wavelength: 210 nm].

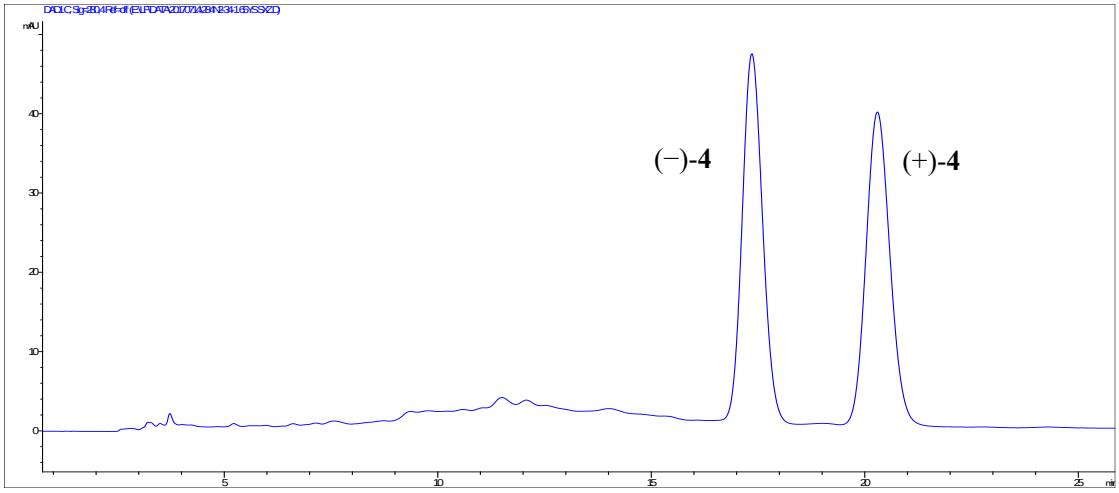

Fig. S4. Chiral HPLC Chromatogram of **4** [column: Phenomenex Cellulose-1 (4.6 × 250 mm, 5 μm), mobile phase: $CH_3CN/H_2O/CF_3COOH$ (65:35:0.1, *V/V/V*), flow rate: 1.0 mL/min, detection wavelength: 280 nm].

7 Quantum chemical ECD calculations of 1−4

7.1 ECD calculation for 1

The conformational analysis of compound **1** was performed in the SYBYL 8.1 program by using MMFF94s molecular force field, which afforded 36 conformers of **1**, with an energy cutoff of 10 kcal mol^{-1} to the global minima. All the obtained conformers were further optimized using DFT at the B3LYP/6-31+G(d) level in acetonitrile by using Gaussian09 software,[3] and 26 conformers of **1** were selected. All of the optimized stable conformers were used for TDDFT computation of the excited stats at the same levels, with the consideration of the first 30 excitations. The overall ECD curves of **1** were weighted by Boltzmann distribution of each conformer (with a half-bandwidth of 0.12 eV), with a UV correction of 3 nm. The calculated ECD spectra of **1** were subsequently compared with the experimental one. The ECD spectra were produced by SpecDis 1.71 software.[4]

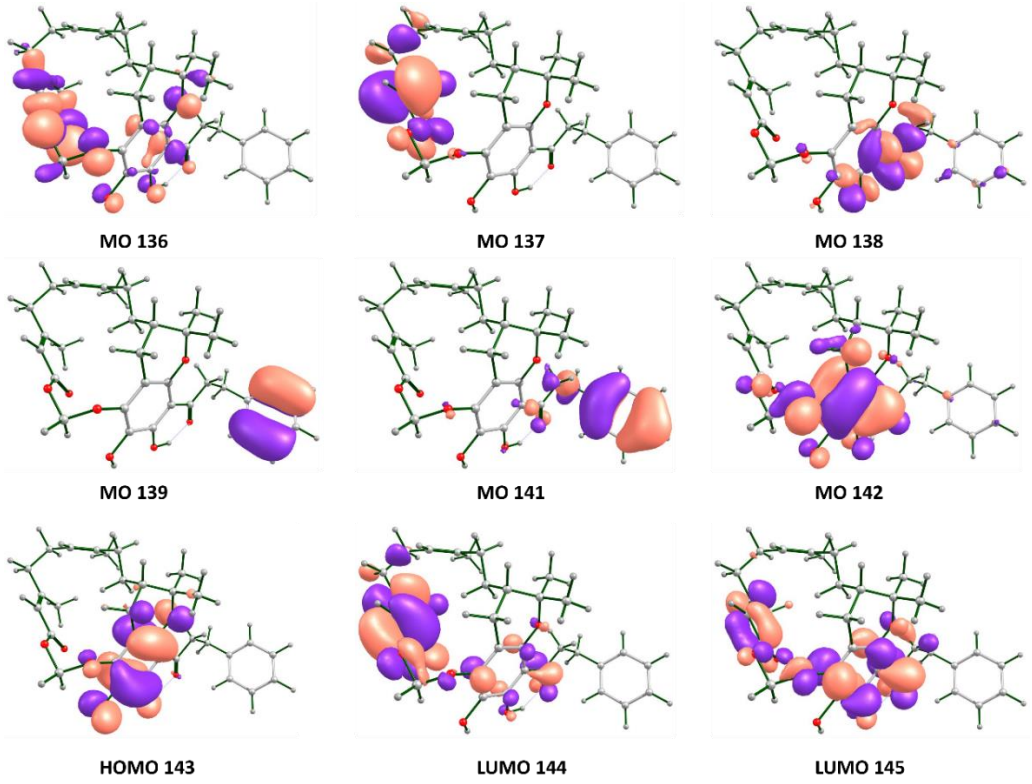

Fig. S8. Key molecular orbitals involved in important transitions regarding the ECD spectra of conformer 6 in acetonitrile at the B3LYP/6-31+G(d) level.

Table S11. Key transitions and their related rotatory and oscillator strengths of conformer 6 of **1** at the B3LYP/6-31+G(d) level in acetonitrile

HOMO is 143					
No.	**Energy (cm^{-1})**	**Wavelength (nm)**	**R(length)**	**Osc. Strength**	**Major contribs**
1	26375.13638	379.1449589	-10.253	0.0209	HOMO->LUMO (96%)
2	27221.21198	367.3605719	17.1003	0.038	HOMO->L+1 (95%)
3	33345.37976	299.8916213	-10.5545	0.0316	H-1->LUMO (94%)
4	34059.18043	293.6065952	13.0796	0.0054	H-5->L+1 (33%), H-2->LUMO (15%), H-2->L+1 (37%)
5	34779.43353	287.5262471	0.721	0.0024	H-3->LUMO (89%)
6	35659.38441	280.4310889	-58.3272	0.2482	H-1->L+1 (78%)
7	36201.38899	276.2324949	12.6078	0.0397	H-5->L+1 (31%), H-2->LUMO (23%), H-2->L+1 (24%)
8	36628.86284	273.0087484	-19.825	0.0099	HOMO->L+2 (76%)
9	37286.2047	268.1957062	0.7312	0.0009	H-8->LUMO (16%), H-7->LUMO (61%)
10	37357.98804	267.6803684	-1.3307	0.0009	H-2->LUMO (59%), H-2->L+1 (35%)
11	37842.72725	264.2515676	-0.43	0.0009	H-4->LUMO (36%), H-4->L+1 (58%)
12	38205.67675	261.7412084	3.0641	0.0057	HOMO->L+3 (82%)
13	38240.35859	261.503824	-1.5511	0.0007	H-3->L+1 (90%)
14	38558.94759	259.3431778	-6.0822	0.0032	HOMO->L+2 (15%), HOMO->L+5 (11%), HOMO->L+6 (15%), HOMO->L+7 (19%), HOMO->L+8 (22%)
15	39009.00496	256.3510659	-0.1235	0.0009	HOMO->L+4 (90%)
16	39491.32451	253.2201724	-2.815	0.0026	HOMO->L+5 (88%)
17	39635.69775	252.2978166	0.0168	0.0001	H-4->LUMO (62%), H-4->L+1 (38%)
18	40004.29312	249.9731709	0.1495	0.0001	HOMO->L+6 (64%), HOMO->L+7 (21%), HOMO->L+8 (10%)
19	40685.02506	245.7906806	3.1524	0.0159	HOMO->L+7 (47%), HOMO->L+8 (39%)
20	42321.524	236.286387	-2.0684	0.0799	HOMO->L+9 (15%), HOMO->L+10 (55%)

21	42433.63506	235.6621106	1.2853	0.0014	H-4->L+5 (23%), H-2->L+3 (14%), H-2->L+4 (41%)
22	42632.85401	234.5608858	2.1533	0.0016	HOMO->L+9 (59%), HOMO->L+10 (13%), HOMO->L+12 (12%)
23	42847.39749	233.3864035	1.7377	0.0008	H-5->LUMO (78%), H-5->L+1 (21%)
24	43347.46123	230.694018	-3.5062	0.0035	HOMO->L+9 (14%), HOMO->L+12 (53%)
25	43569.2637	229.5196005	35.5641	0.0347	H-8->LUMO (10%), H-6->LUMO (16%), H-1->L+2 (20%)
26	43611.20453	229.2988719	51.176	0.0205	H-6->LUMO (14%), H-1->L+2 (54%)
27	43762.83676	228.5043827	-11.1155	0.0594	H-7->L+1 (12%), H-6->LUMO (23%), H-6->L+1 (18%), HOMO->L+11 (21%)
28	44224.1859	226.1206125	68.296	0.0627	H-7->LUMO (14%), H-6->L+1 (28%), HOMO->L+11 (22%)
29	44572.61741	224.3529903	6.5988	0.0021	HOMO->L+13 (65%), HOMO->L+15 (14%)
30	44819.42307	223.117553	0.3874	0.0053	H-8->LUMO (34%), H-7->L+1 (56%)

Table S12. Cartesian coordinates of conformer 6 of **1**

Standard orientation:					
Center Number	**Atomic Number**	**Atomic Type**	**Coordinates (Angstroms)**		
			X	**Y**	**Z**
1	6	0	-2.010541	2.962915	-1.239329
2	8	0	-0.914152	2.412593	-1.990579
3	8	0	-3.109797	2.040766	-1.220526
4	6	0	-5.895511	0.832361	0.600509
5	6	0	-5.095624	1.261022	-0.39641
6	6	0	-4.060576	2.315874	-0.294148
7	6	0	-5.332251	-2.166384	0.111335
8	6	0	-6.559871	-1.645512	0.809339
9	6	0	-6.94169	-0.236881	0.319706
10	6	0	0.003801	1.810772	-1.168036
11	6	0	0.117729	0.409251	-1.172929
12	6	0	-0.736451	-0.42194	-2.092235
13	6	0	-0.967217	-1.81993	-1.501793
14	6	0	-1.978322	-1.701643	-0.326463
15	6	0	-2.981775	-2.862794	-0.253728
16	6	0	-4.144381	-2.500535	0.653742
17	6	0	0.843632	2.573682	-0.362253
18	6	0	1.772601	1.955717	0.465579
19	6	0	1.905224	0.559634	0.48826
20	6	0	1.054861	-0.215159	-0.321588
21	8	0	1.123492	-1.575406	-0.183485
22	6	0	0.411203	-2.415067	-1.109338
23	6	0	-3.836151	-2.503955	2.125846
24	6	0	-5.855641	1.325738	2.021522
25	8	0	-4.073186	3.262326	0.472823
26	6	0	0.258992	-3.770784	-0.40077
27	6	0	1.318935	-2.644067	-2.335233
28	8	0	0.773386	3.940959	-0.354988
29	8	0	2.528314	2.793624	1.256557
30	6	0	2.95894	0.000206	1.385453
31	8	0	3.347397	0.734659	2.300737
32	6	0	3.539385	-1.38143	1.145056
33	6	0	4.963763	-1.523754	1.688043
34	6	0	5.980721	-0.78921	0.84626
35	6	0	6.442106	-1.344727	-0.355496
36	6	0	7.367039	-0.657925	-1.14385
37	6	0	7.837811	0.590288	-0.740283
38	6	0	7.384459	1.152589	0.451662
39	6	0	6.46027	0.466628	1.241452
40	1	0	-1.722789	3.249324	-0.21971
41	1	0	-2.33502	3.863646	-1.771671
42	1	0	-5.175589	0.812808	-1.383214
43	1	0	-5.431477	-2.214842	-0.9733
44	1	0	-6.453168	-1.63951	1.89671
45	1	0	-7.389171	-2.32868	0.588561

46	1	0	-7.885934	0.062209	0.792897
47	1	0	-7.157969	-0.279121	-0.756673
48	1	0	-1.703714	0.052861	-2.287988
49	1	0	-0.235317	-0.489528	-3.064969
50	1	0	-1.418102	-2.439046	-2.288396
51	1	0	-1.452032	-1.603889	0.630665
52	1	0	-2.557897	-0.7762	-0.440531
53	1	0	-2.505871	-3.779594	0.108286
54	1	0	-3.351097	-3.090142	-1.261673
55	1	0	-3.180804	-1.665504	2.381257
56	1	0	-4.726401	-2.437198	2.754561
57	1	0	-3.328834	-3.434786	2.40157
58	1	0	-4.975556	1.930453	2.248469
59	1	0	-6.746953	1.923919	2.235945
60	1	0	-5.833628	0.482619	2.71948
61	1	0	-0.217668	-3.661219	0.578799
62	1	0	-0.317374	-4.479384	-1.004098
63	1	0	1.24026	-4.215783	-0.195171
64	1	0	1.614047	-1.706018	-2.815364
65	1	0	0.830074	-3.279456	-3.080895
66	1	0	2.258819	-3.124199	-2.036914
67	1	0	1.465699	4.212562	0.283959
68	1	0	3.023586	2.206441	1.885878
69	1	0	3.541927	-1.605305	0.073513
70	1	0	2.892411	-2.100133	1.660492
71	1	0	5.236162	-2.586976	1.705551
72	1	0	5.023216	-1.184942	2.729747
73	1	0	6.082704	-2.316933	-0.684548
74	1	0	7.719661	-1.096625	-2.073327
75	1	0	8.557048	1.12497	-1.354525
76	1	0	7.749023	2.126589	0.766494
77	1	0	6.111289	0.92056	2.166543

7.2 ECD calculation for 2

The conformational analysis of compound **2** was performed in the SYBYL 8.1 program by using MMFF94s molecular force field, which afforded 48 conformers of **2**, with an energy cutoff of 10 kcal mol^{-1} to the global minima. All the obtained conformers were further optimized using DFT at the CAM-B3LYP/6-31+G(d) level in acetonitrile by using Gaussian09 software,[3] and 22 conformers of **2** were selected. All of the optimized stable conformers were used for TDDFT computation of the excited stats at the same levels, with the consideration of the first 30 excitations. The overall ECD curves of **2** were weighted by Boltzmann distribution of each conformer (with a half-bandwidth of 0.15 eV), with a UV correction of 6 nm. The calculated ECD spectra of

2 were subsequently compared with the experimental one. The ECD spectra were produced by SpecDis 1.71 software.[4]

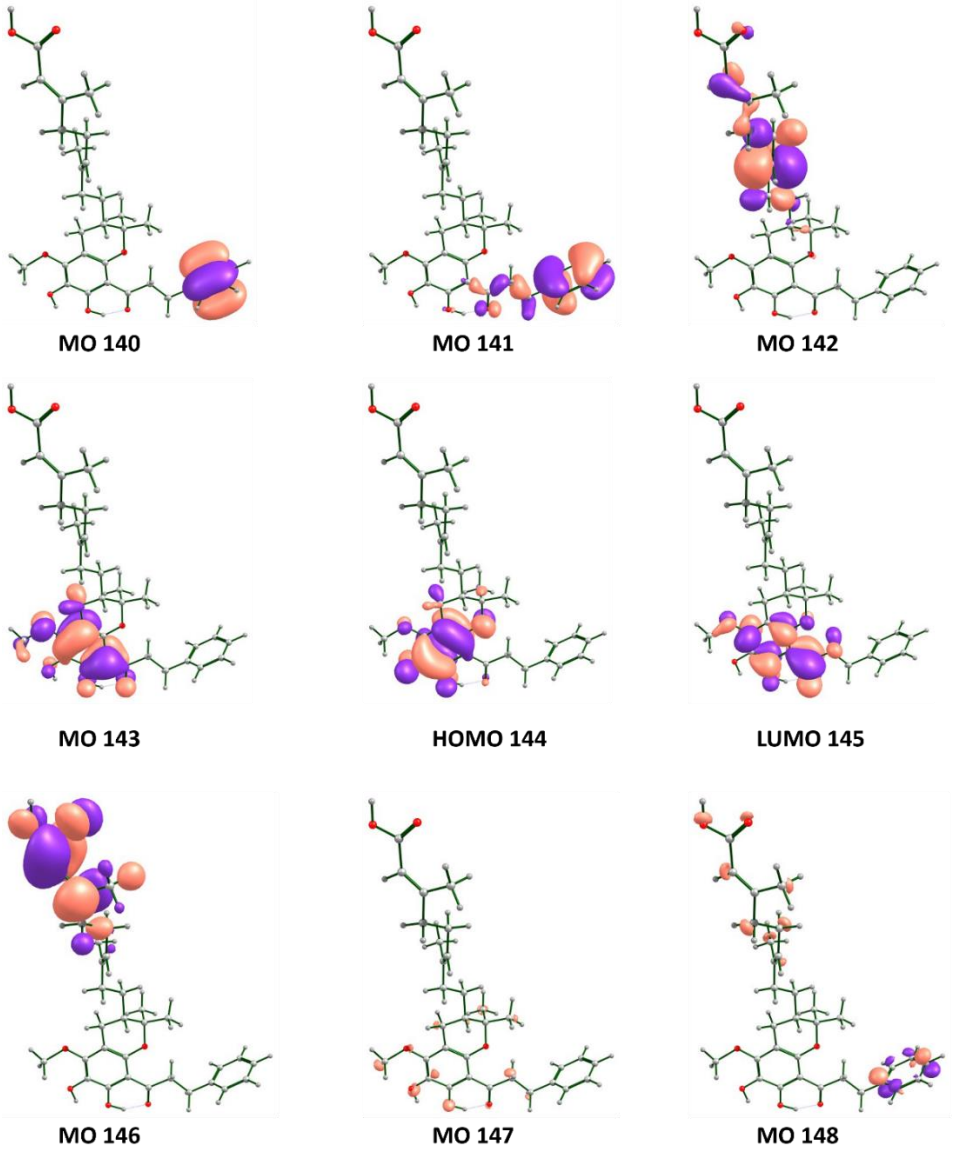

Fig. S9. Key molecular orbitals involved in important transitions regarding the ECD spectra of conformer 4 in acetonitrile at the CAM-B3LYP/6-31+G(d) level.

Table S13. Key transitions and their related rotatory and oscillator strengths of conformer 4 of **2** at the CAM-B3LYP/6-31+G(d) level in acetonitrile

HOMO is 144					
No.	**Energy (cm^{-1})**	**Wavelength (nm)**	**R (length)**	**Osc. Strength**	**Major contribs**
1	31102.35189	321.519094	4.0093	0.127	HOMO->LUMO (95%)
2	36787.75406	271.8295872	5.3204	0.0004	H-6->LUMO (70%), H-3->LUMO (14%)
3	37421.70584	267.22459	-16.6878	0.4747	H-1->LUMO (92%)
4	41159.27907	242.9585801	0.064	0.0001	HOMO->L+2 (59%), HOMO->L+6 (18%)
5	42164.24588	237.167766	37.2435	0.0322	H-8->L+1 (79%)
6	43979.7999	227.3771145	-0.055	0.0019	H-4->L+4 (28%), H-3->L+5 (49%)
7	45741.31478	218.6207381	-108.0944	0.5982	H-8->L+1 (11%), H-5->L+1 (39%), H-2->L+1 (45%)
8	46855.16644	213.4236363	-45.304	0.2497	HOMO->L+14 (11%), HOMO->L+16 (44%)
9	47539.1246	210.3530531	-1.7921	0.0386	H-1->L+2 (46%), H-1->L+6 (11%), HOMO->L+16 (10%)
10	48389.23297	206.6575431	-7.6506	0.0069	H-1->L+2 (11%), HOMO->L+8 (10%), HOMO->L+11 (12%)
11	48870.74596	204.6213906	45.734	0.0163	H-7->LUMO (24%), H-3->LUMO (44%)
12	48960.2735	204.247225	-12.6997	0.03	H-4->L+5 (25%), H-3->LUMO (12%), H-3->L+4 (35%)
13	49220.79058	203.16618	-37.0296	0.0467	H-7->LUMO (17%), H-3->LUMO (17%)
14	49319.19022	202.7608311	-13.1262	0.1291	H-5->L+1 (44%), H-2->L+1 (34%)
15	49827.31951	200.6931157	-6.5847	0.0759	H-7->LUMO (17%), HOMO->L+9 (22%)
16	50073.31862	199.707155	-11.8478	0.0467	HOMO->L+3 (13%), HOMO->L+6 (19%), HOMO->L+7 (10%), HOMO->L+10 (12%)
17	50241.88849	199.0371043	-0.7699	0.0012	HOMO->L+1 (96%)
18	50704.04418	197.2229269	-45.4341	0.0365	H-2->L+2 (15%), H-2->L+3 (31%), H-2->L+7 (13%)
19	50825.02734	196.7534603	40.66	0.128	H-1->L+16 (24%), HOMO->L+8 (12%), HOMO->L+29 (13%)
20	51648.51942	193.6163924	-8.6092	0.0136	H-2->LUMO (74%)

21	52368.77252	190.9534923	-22.4948	0.0731	H-4->LUMO (71%)
22	52640.58136	189.9675068	-3.1347	0.0048	H-4->LUMO (19%), H-3->L+2 (23%), H-3->L+6 (30%)
23	52818.82989	189.3264205	-1.3898	0.0007	HOMO->L+3 (15%), HOMO->L+4 (34%), HOMO->L+6 (11%)
24	53301.14944	187.6132148	165.0636	0.2956	H-2->L+6 (14%), H-2->L+8 (29%), H-2->L+9 (19%)
25	53574.57139	186.6557163	2.2318	0.0156	HOMO->L+2 (15%), HOMO->L+4 (34%), HOMO->L+7 (12%)
26	53708.45943	186.1904085	-65.5898	0.0987	H-1->L+16 (10%), HOMO->L+5 (39%)
27	53861.70477	185.6606664	9.3274	0.02	H-1->L+3 (14%), H-1->L+7 (15%)
28	54231.91325	184.3932733	13.2047	0.0129	HOMO->L+3 (11%), HOMO->L+10 (11%), HOMO->L+17 (25%)
29	54275.46719	184.2453049	10.6885	0.0216	H-4->L+2 (23%), H-4->L+3 (11%), H-4->L+6 (37%)
30	54625.51181	183.0646463	160.2453	0.4609	H-4->L+4 (40%), H-3->L+5 (30%)
31	54656.96744	182.9592908	0.3736	0.0108	H-1->L+8 (23%)
32	54823.9242	182.40212	-78.7536	0.0251	H-2->L+8 (16%), H-2->L+11 (16%), H-2->L+15 (10%)
33	54877.15679	182.2251841	-19.417	0.0317	HOMO->L+8 (10%)
34	55203.00478	181.1495595	-60.6351	0.0594	HOMO->L+5 (16%), HOMO->L+29 (14%)
35	55411.90238	180.4666429	-46.8327	0.878	H-4->L+5 (50%), H-3->L+4 (18%)
36	55558.69529	179.9898278	17.1017	0.021	H-9->LUMO (60%)
37	55774.04532	179.2948663	-13.7356	0.0238	HOMO->L+12 (16%)
38	55858.73353	179.0230348	10.3084	0.0123	H-1->L+1 (61%)
39	55878.09084	178.9610176	3.7799	0.0016	H-1->L+1 (33%)
40	55924.871	178.8113199	28.6765	0.0964	HOMO->L+29 (10%)
41	56239.42723	177.8111992	-4.5521	0.0125	H-5->L+3 (22%), H-2->L+7 (13%)
42	56930.64437	175.6523242	23.3091	0.0647	
43	56975.81142	175.5130774	-5.2603	0.0177	H-6->L+2 (13%), H-3->L+2 (12%), H-3->L+10 (22%)

44	57780.75274	173.0680119	10.0792	0.155	H-2->L+20 (11%)
45	57948.51606	172.5669729	42.7462	0.069	HOMO->L+3 (16%)
46	58075.14511	172.1907019	5.6957	0.0051	H-1->L+4 (19%)
47	58270.33128	171.6139205	0.0093	0.0058	H-1->L+4 (32%)
48	58480.03543	170.9985284	-2.0121	0.0048	H-3->L+9 (15%), H-3->L+12 (28%), H-3->L+14 (16%)
49	58579.24162	170.7089358	55.5155	0.0332	H-3->L+10 (14%)
50	58709.90344	170.3290146	-40.0414	0.0465	H-2->L+2 (11%)

Table S14. Cartesian coordinates of conformer 4 of **2**

Standard orientation:					
Center Number	**Atomic Number**	**Atomic Type**	**Coordinates (Angstroms)**		
			X	**Y**	**Z**
1	6	0	2.089235	3.546557	0.019251
2	6	0	3.418503	3.889621	-0.211228
3	6	0	4.389004	2.897304	-0.367129
4	6	0	4.076072	1.53253	-0.28543
5	6	0	2.737658	1.177692	-0.051772
6	6	0	1.745161	2.172668	0.076043
7	6	0	5.211204	0.565004	-0.444665
8	6	0	5.017708	-0.925378	-0.253781
9	8	0	6.31398	1.048896	-0.726773
10	8	0	1.035223	4.40405	0.199444
11	8	0	5.669151	3.362296	-0.601576
12	6	0	6.340106	-1.687895	-0.3563
13	6	0	6.218393	-3.717588	1.142735
14	6	0	6.137429	-3.167191	-0.143555
15	6	0	5.830965	-4.004826	-1.224507
16	6	0	5.619586	-5.369893	-1.023189
17	6	0	5.708181	-5.908629	0.259324
18	6	0	6.006736	-5.082934	1.341928
19	6	0	0.302165	1.786014	0.301892
20	8	0	2.43287	-0.150886	0.01152
21	6	0	1.182364	-0.552295	0.603974
22	6	0	0.027729	0.302438	0.02663
23	6	0	1.032988	-2.029156	0.194657
24	6	0	1.319552	-0.49781	2.135432
25	8	0	3.861896	5.182208	-0.305416
26	6	0	-9.344334	-0.220497	-0.020719
27	6	0	-8.48505	-0.820916	-0.867402
28	6	0	-7.101166	-0.232241	-1.077905
29	6	0	-5.993575	-1.121993	-0.503166
30	6	0	-4.637388	-0.500665	-0.698444
31	6	0	-3.881681	0.124814	0.225906
32	6	0	-2.515036	0.669636	-0.145486
33	6	0	-4.312063	0.375465	1.646381
34	6	0	-10.699336	-0.693026	0.319741
35	6	0	-8.786582	-2.05216	-1.679821
36	8	0	-11.225465	-1.753142	0.045892
37	8	0	-11.331557	0.253162	1.039247
38	6	0	-1.375448	-0.111481	0.526363
39	6	0	1.283603	5.801855	0.212604
40	1	0	0.046926	0.175071	-1.0666
41	1	0	4.584642	-1.09903	0.737682
42	1	0	4.334247	-1.291261	-1.027967
43	1	0	6.239545	2.55619	-0.718729
44	1	0	6.804191	-1.519933	-1.336886
45	1	0	7.059481	-1.306826	0.380213

46	1	0	6.446316	-3.085114	1.997451
47	1	0	5.754321	-3.597817	-2.230018
48	1	0	5.384555	-6.012682	-1.867184
49	1	0	5.543396	-6.9712	0.415196
50	1	0	6.073734	-5.502038	2.342228
51	1	0	0.033256	2.039505	1.334994
52	1	0	-0.331318	2.383732	-0.364712
53	1	0	0.184439	-2.516058	0.68389
54	1	0	1.936983	-2.595692	0.450266
55	1	0	0.912137	-2.122152	-0.890783
56	1	0	2.196893	-1.069429	2.461525
57	1	0	1.474832	0.521871	2.501086
58	1	0	0.4403	-0.911042	2.63894
59	1	0	4.824942	5.092828	-0.473816
60	1	0	-9.046029	0.685057	0.500999
61	1	0	-7.037695	0.763073	-0.617603
62	1	0	-6.940745	-0.072823	-2.152324
63	1	0	-5.989963	-2.095833	-1.00883
64	1	0	-6.188542	-1.338784	0.552575
65	1	0	-4.240929	-0.605852	-1.708211
66	1	0	-2.375625	0.639643	-1.233653
67	1	0	-2.475795	1.728003	0.137898
68	1	0	-5.381884	0.217455	1.804398
69	1	0	-3.766974	-0.280736	2.331779
70	1	0	-4.107174	1.414461	1.926348
71	1	0	-8.386464	-2.942192	-1.184603
72	1	0	-9.854247	-2.198654	-1.856589
73	1	0	-8.32628	-1.976432	-2.671278
74	1	0	-12.213687	-0.127316	1.231223
75	1	0	-1.533368	-1.178075	0.331412
76	1	0	-1.435349	0.024545	1.612608
77	1	0	1.963792	6.079084	1.024036
78	1	0	1.638474	6.150607	-0.762074
79	1	0	0.329802	6.303037	0.406222

7.3 ECD calculation for 3

The conformational analysis of compound **3** was performed in the SYBYL 8.1 program by using MMFF94s molecular force field, which afforded 25 conformers of **3**, with an energy cutoff of 10 kcal mol^{-1} to the global minima. All the obtained conformers were further optimized using DFT at the CAM-B3LYP/6-31+G(d) level in acetonitrile by using Gaussian09 software,[3] and 12 conformers of **3** were selected. All of the optimized stable conformers were used for TDDFT computation of the excited stats at the same levels, with the consideration of the first 30 excitations. The overall ECD curves of **3** were weighted by Boltzmann distribution of each conformer (with a half-bandwidth of 0.10 eV), with a UV correction of 5 nm. The calculated ECD spectra of **3** were subsequently compared with the experimental one. The ECD spectra were produced by SpecDis 1.71 software.[4]

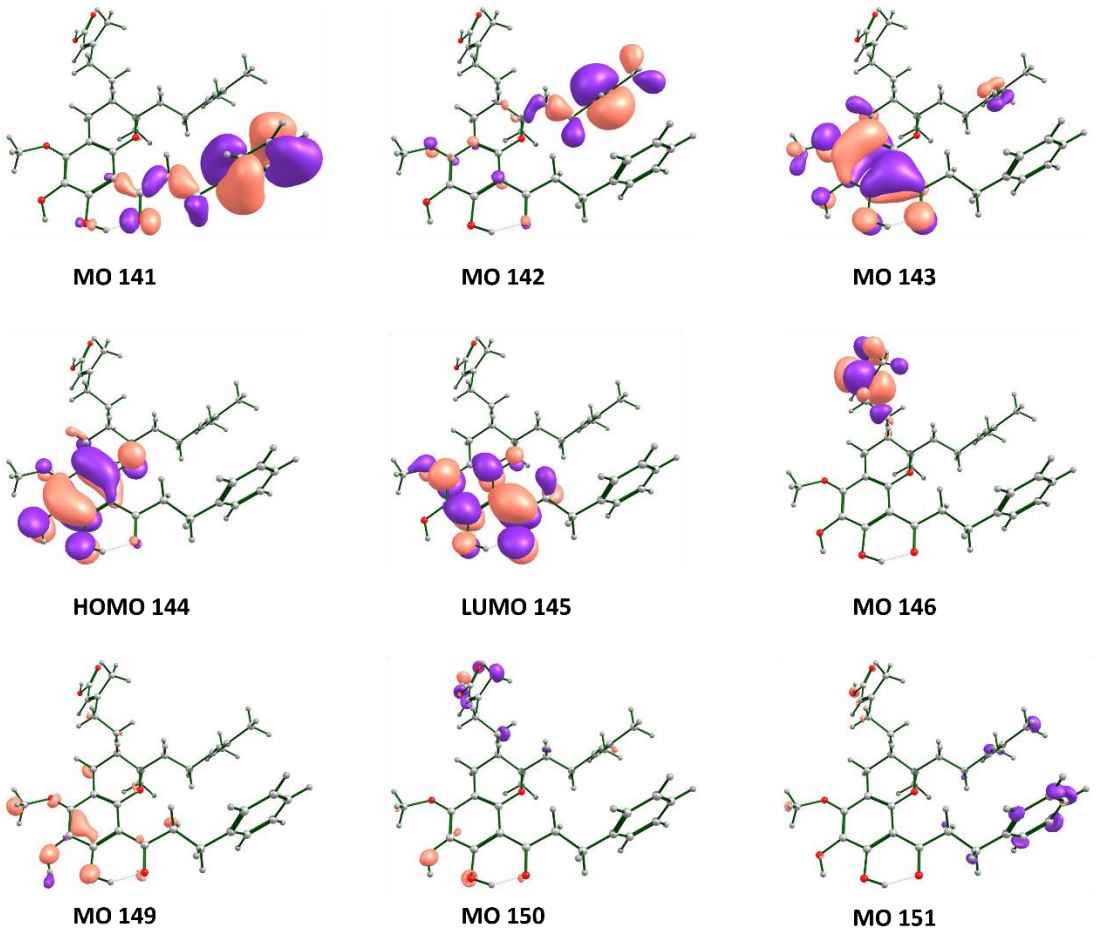

Fig. S10. Key molecular orbitals involved in important transitions regarding the ECD spectra of conformer 3 in acetonitrile at the CAM-B3LYP/6-31+G(d) level.

Table S15. Key transitions and their related rotatory and oscillator strengths of conformer 3 of **3** at the CAM-B3LYP/6-31+G(d) level in acetonitrile.

HOMO is 144					
No.	**Energy (cm^{-1})**	**Wavelength (nm)**	**R(length)**	**Osc. Strength**	**Major contribs**
1	26838.09863	372.6046372	10.3484	0.0875	HOMO->LUMO (97%)
2	30636.16343	326.4116286	-0.0339	0.0004	HOMO->L+1 (100%)
3	33809.95511	295.7708748	11.358	0.0083	H-6->LUMO (41%), H-3->LUMO (54%)
4	34098.70159	293.2662985	-9.7133	0.2027	H-2->LUMO (34%), H-1->LUMO (64%)
5	34389.06119	290.7901424	-19.6515	0.2279	H-2->LUMO (64%), H-1->LUMO (31%)
6	36089.27793	277.090609	0.072	0.0014	H-1->L+1 (100%)
7	36453.03397	274.3255886	0.1812	0.0008	H-2->L+1 (100%)
8	37717.71132	265.1274335	-1.1484	0.0009	H-6->LUMO (54%), H-3->LUMO (43%)
9	37916.12371	263.7400404	-1.1852	0.0004	HOMO->L+4 (83%), HOMO->L+5 (12%)
10	38689.6094	258.4673289	-0.177	0.0026	H-4->LUMO (100%)
11	39264.68271	254.6817982	-0.2796	0.0004	H-8->L+1 (82%), H-7->L+1 (15%)
12	39629.24531	252.3388957	0.4983	0.0028	HOMO->L+2 (98%)
13	39654.2485	252.1797885	0.1636	0.0002	HOMO->L+3 (99%)
14	39990.5817	250.0588782	-0.2517	0.0014	H-3->L+1 (100%)
15	41701.28364	239.8007717	8.9368	0.032	H-7->LUMO (23%), H-5->LUMO (65%)
16	42142.46892	237.2903216	-0.0328	0	H-4->L+1 (100%)
17	42239.25545	236.7465973	-14.1258	0.0204	HOMO->L+4 (11%), HOMO->L+5 (44%), HOMO->L+6 (14%), HOMO->L+11 (11%)
18	42535.26092	235.0990633	12.7086	0.0575	H-5->LUMO (14%), HOMO->L+5 (21%), HOMO->L+6 (12%), HOMO->L+7 (23%)
19	42647.37199	234.4810368	1.3087	0.0013	H-4->L+3 (38%), H-3->L+2 (51%)
20	42940.9578	232.8778982	9.8592	0.0216	H-7->LUMO (21%), HOMO->L+6 (47%)
21	43452.31331	230.1373446	-23.6038	0.0175	H-7->LUMO (29%), HOMO->L+7 (16%), HOMO->L+9 (15%)

22	43741.86635	228.6139307	0.7419	0.0004	H-1->L+4 (74%)
23	43852.3643	228.0378757	-0.032	0.0028	H-2->L+2 (78%)
24	43995.12444	227.2979137	-0.8917	0.0007	H-2->L+3 (81%)
25	44104.81584	226.7326098	-52.0869	0.5718	H-5->L+1 (92%)
26	44304.03479	225.7130767	14.0765	0.0879	HOMO->L+7 (11%), HOMO->L+9 (52%)
27	44651.65974	223.9558408	-1.1782	0.002	HOMO->L+5 (12%), HOMO->L+10 (29%), HOMO->L+11 (33%)
28	44982.34706	222.3094314	4.2001	0.0052	HOMO->L+8 (69%)
29	45083.16636	221.8122818	0.254	0.0002	H-1->L+3 (86%)
30	45152.53004	221.4715319	-0.3199	0.0043	H-1->L+2 (81%)
31	45498.54189	219.7872631	1.9071	0.0028	H-2->L+4 (25%), H-2->L+6 (14%), HOMO->L+10 (21%), HOMO->L+11 (10%)
32	45534.83684	219.6120749	13.7761	0.0157	H-2->L+4 (21%), H-2->L+6 (10%), HOMO->L+10 (25%), HOMO->L+11 (12%)
33	46518.83325	214.9666985	21.1141	0.1186	H-8->LUMO (34%)
34	46550.28887	214.8214381	-17.7008	0.0053	H-6->L+1 (88%)
35	46746.2816	213.9207582	-12.8576	0.1369	H-8->LUMO (40%), HOMO->L+7 (11%), HOMO->L+12 (14%)
36	47051.96572	212.5309718	4.9202	0.0159	HOMO->L+12 (45%), HOMO->L+15 (34%)
37	47129.39495	212.1818031	-35.3934	0.0118	H-8->L+1 (13%), H-7->L+1 (76%)
38	47316.51558	211.3426967	9.3763	0.0246	H-4->L+2 (24%), H-3->L+3 (60%)
39	47340.71221	211.2346759	1.8049	0.0012	HOMO->L+13 (48%), HOMO->L+14 (22%)
40	47768.18606	209.3443529	1.5288	0.0046	H-2->L+4 (45%), H-2->L+5 (12%), H-2->L+6 (27%)
41	47860.93982	208.9386468	-1.817	0.0009	H-9->LUMO (73%), H-8->LUMO (12%)
42	47953.69358	208.5345102	3.4339	0.0082	HOMO->L+14 (48%)
43	48008.53928	208.2962771	-1.3812	0.0008	H-1->L+5 (62%), H-1->L+10 (10%)
44	48077.0964	207.9992501	15.1731	0.0347	H-1->L+6 (45%), HOMO->L+15 (14%)

45	48220.66309	207.3799769	-15.8423	0.0116	H-3->L+4 (29%), H-3->L+6 (22%), H-2->L+5 (15%), H-2->L+6 (13%)
46	48288.41366	207.0890146	8.1383	0.0372	H-1->L+6 (19%), HOMO->L+17 (15%)
47	48457.79009	206.3651681	17.509	0.0163	H-3->L+4 (21%), H-3->L+6 (15%), H-2->L+5 (25%), H-2->L+6 (20%)
48	49078.837	203.7538094	-6.9608	0.0079	H-2->L+9 (67%), H-1->L+9 (15%)
49	49155.45968	203.4362015	-3.6081	0.005	HOMO->L+16 (56%)
50	49340.16064	202.6746543	-7.0293	0.013	H-2->L+9 (13%), H-1->L+9 (47%)

Table S16. Cartesian coordinates of conformer 3 of **3**

Standard orientation:					
Center Number	**Atomic Number**	**Atomic Type**	**Coordinates (Angstroms)**		
			X	**Y**	**Z**
1	6	0	-1.174786	3.850742	0.037711
2	6	0	-0.095722	4.726919	0.045972
3	6	0	1.210311	4.236516	0.009969
4	6	0	1.490968	2.860502	-0.020557
5	6	0	0.406582	1.96296	-0.010735
6	6	0	-0.91597	2.456436	-0.013701
7	6	0	2.941782	2.478727	-0.054879
8	6	0	3.373374	1.03306	-0.080677
9	8	0	3.763785	3.402413	-0.056681
10	8	0	-2.504941	4.18126	0.072644
11	8	0	-0.224918	6.089847	0.082380
12	6	0	-2.870064	5.551174	0.148526
13	8	0	2.194196	5.207947	0.011778
14	6	0	4.893154	0.876226	-0.151380
15	6	0	5.278898	-0.581582	-0.203912
16	6	0	5.440251	-1.2298	-1.435979
17	6	0	5.750893	-2.589937	-1.484019
18	6	0	5.89774	-3.314812	-0.302666
19	6	0	5.736171	-2.680337	0.927781
20	6	0	5.427813	-1.319852	0.978068
21	8	0	0.670308	0.620186	-0.024522
22	6	0	-2.087755	1.507718	-0.055842
23	6	0	-1.691669	0.070927	-0.408655
24	6	0	-2.871981	-0.902755	-0.167779
25	6	0	-0.377099	-0.311303	0.333966
26	6	0	0.111175	-1.709704	-0.159665
27	6	0	-4.13925	-0.545022	-0.961259
28	6	0	-5.232792	-1.585746	-0.798051
29	6	0	-6.34049	-1.286901	-0.091207
30	6	0	-7.461784	-2.203473	0.187329
31	6	0	1.456892	-2.18171	0.405263
32	6	0	1.870116	-3.49945	-0.191545
33	6	0	1.763793	-4.721402	0.364469
34	6	0	2.281341	-5.93817	-0.355508
35	6	0	1.137315	-5.007963	1.700205
36	8	0	-7.536028	-3.397971	-0.021137
37	6	0	-4.982935	-2.896279	-1.496317
38	8	0	-8.467235	-1.514205	0.758742
39	6	0	-0.519302	-0.326458	1.868616
40	1	0	3.010292	0.558269	0.83711
41	1	0	2.928443	0.554813	-0.960068
42	1	0	0.700608	6.417296	0.072094
43	1	0	-3.963181	5.597986	0.184464
44	1	0	-2.497525	6.012756	1.068275
45	1	0	-2.553636	6.096624	-0.745888

46	1	0	3.062695	4.724236	-0.016472
47	1	0	5.292165	1.396037	-1.031915
48	1	0	5.369552	1.351161	0.715958
49	1	0	5.318943	-0.679601	-2.366019
50	1	0	5.873918	-3.084893	-2.443445
51	1	0	6.134391	-4.374463	-0.340433
52	1	0	5.845194	-3.246472	1.848799
53	1	0	5.295349	-0.840578	1.94513
54	1	0	-2.597281	1.538543	0.91535
55	1	0	-2.794803	1.864643	-0.814795
56	1	0	-1.466406	0.062449	-1.486145
57	1	0	-3.118506	-0.934664	0.900538
58	1	0	-2.569427	-1.914867	-0.452196
59	1	0	0.195584	-1.680095	-1.254841
60	1	0	-0.633764	-2.475135	0.084865
61	1	0	-3.899057	-0.440278	-2.026621
62	1	0	-4.512857	0.433162	-0.636339
63	1	0	-6.450077	-0.301778	0.35434
64	1	0	2.240009	-1.461529	0.164152
65	1	0	1.426591	-2.242052	1.496186
66	1	0	2.332232	-3.415483	-1.175062
67	1	0	3.039084	-6.443365	0.252476
68	1	0	1.464438	-6.640946	-0.549238
69	1	0	2.741113	-5.688686	-1.317652
70	1	0	0.370066	-5.782901	1.596509
71	1	0	1.896111	-5.366467	2.403192
72	1	0	0.648762	-4.137912	2.145245
73	1	0	-4.390308	-3.560487	-0.859914
74	1	0	-5.904531	-3.409009	-1.781138
75	1	0	-4.430558	-2.734043	-2.428562
76	1	0	-9.167498	-2.180487	0.918222
77	1	0	-0.949733	0.602968	2.253581
78	1	0	-1.148371	-1.154859	2.208765
79	1	0	0.458836	-0.411205	2.354607

7.4 ECD calculation for 4

The conformational analysis of compound **4** was performed in the SYBYL 8.1 program by using MMFF94s molecular force field, which afforded 38 conformers of **4**, with an energy cutoff of 10 kcal mol^{-1} to the global minima. All the obtained conformers were further optimized using DFT at the CAM-B3LYP/6-31+G(d) level in acetonitrile by using Gaussian09 software,[3] and 16 conformers of **4** were selected. All of the optimized stable conformers were used for TDDFT computation of the excited stats at the same levels, with the consideration of the first 30 excitations. The overall ECD curves of **4** were weighted by Boltzmann distribution of each conformer (with a half-bandwidth of 0.18 eV), with a UV correction of 3 nm. The calculated ECD spectra of **4** were subsequently compared with the experimental one. The ECD spectra were produced by SpecDis 1.71 software.[4]

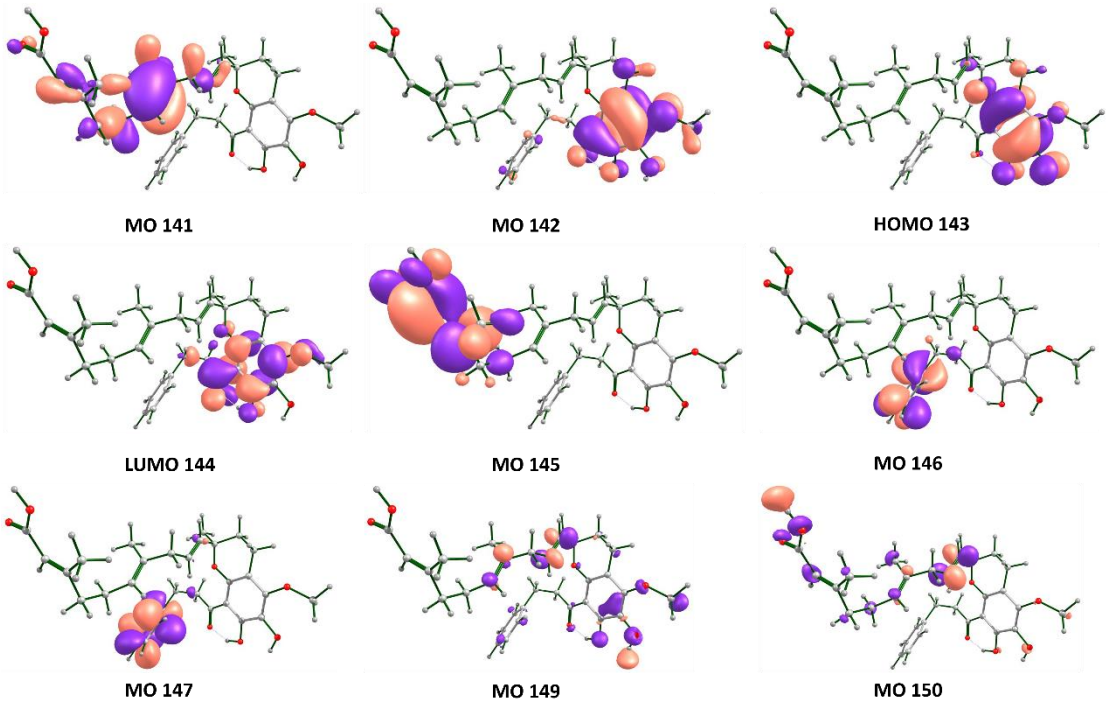

Fig. S11. Key molecular orbitals involved in important transitions regarding the ECD spectra of conformer 2 in acetonitrile at the CAM-B3LYP/6-31+G(d) level.

Table S15. Key transitions and their related rotatory and oscillator strengths of conformer 2 of **4** at the CAM-B3LYP/6-31+G(d) level in acetonitrile.

HOMO is 143					
No.	**Energy (cm^{-1})**	**Wavelength (nm)**	**R (length)**	**Osc. Strength**	**Major contribs**
1	26094.45544	383.2231725	20.0537	0.0694	HOMO->LUMO (98%)
2	31368.51485	318.790993	0.0369	0	HOMO->L+1 (100%)
3	32587.21859	306.8687796	-64.9959	0.1054	H-7->LUMO (31%), H-3->LUMO (44%), H-1->LUMO (23%)
4	33659.12943	297.0962164	50.1804	0.3177	H-7->LUMO (19%), H-1->LUMO (71%)
5	34258.39937	291.8992184	-0.6008	0.0011	H-2->LUMO (98%)
6	34877.02662	286.7216896	15.7157	0.0604	H-2->L+1 (99%)
7	36313.50006	275.3796793	-0.9744	0.0098	H-7->LUMO (43%), H-3->LUMO (46%)
8	36731.29525	272.2474101	-2.6742	0.0027	H-4->LUMO (97%)
9	36983.74679	270.3890457	0.0157	0	H-1->L+1 (100%)
10	37028.91384	270.0592311	-0.6432	0.0006	H-5->LUMO (93%)
11	37940.32034	263.5718389	-2.2289	0.0003	HOMO->L+2 (25%), HOMO->L+5 (61%)
12	38824.30399	257.5706187	-1.5714	0.0004	HOMO->L+2 (73%), HOMO->L+5 (19%)
13	39211.45012	255.0275486	1.1279	0.0034	HOMO->L+3 (64%), HOMO->L+4 (29%)
14	39611.50112	252.4519323	-1.1338	0.0005	HOMO->L+3 (32%), HOMO->L+4 (53%), HOMO->L+5 (11%)
15	39663.1206	252.1233793	0.1883	0.0002	H-3->L+1 (100%)
16	40540.65182	246.6659896	-0.41	0	H-9->L+1 (97%)
17	40703.57581	245.6786609	2.5421	0.0036	H-4->L+1 (99%)
18	41484.3205	241.0549306	0.9273	0.0018	H-5->L+1 (99%)
19	41985.99736	238.1746446	16.1498	0.0541	H-8->LUMO (69%), HOMO->L+9 (16%)
20	42485.25455	235.3757817	-1.2822	0.001	H-6->LUMO (20%), HOMO->L+6 (36%), HOMO->L+7 (18%)
21	42549.7789	235.0188475	-1.4433	0.0087	H-6->LUMO (72%), HOMO->L+6 (10%)
22	42616.72292	234.6496707	-0.2967	0.0019	H-5->L+2 (23%), H-5->L+3 (12%), H-3->L+2 (17%), H-3->L+3 (26%)
23	42920.79394	232.9873025	-4.2961	0.0067	HOMO->L+6 (24%), HOMO->L+7 (48%)
24	43272.45167	231.0939088	-28.0881	0.0403	H-8->LUMO (14%), HOMO->L+7 (16%), HOMO->L+9 (25%), HOMO->L+10 (13%)
25	43816.87591	228.2225693	1.3034	0.0037	H-1->L+2 (37%), H-1->L+5 (28%)

26	44138.69113	226.5585985	-22.7301	0.0485	H-1->L+2 (14%), HOMO->L+8 (55%)
27	44466.95878	224.8860789	-17.1936	0.0077	H-1->L+2 (31%), H-1->L+3 (14%), H-1->L+5 (39%)
28	44557.29288	224.4301517	55.2823	0.396	H-6->L+1 (34%), H-2->L+3 (12%), H-2->L+4 (41%)
29	44811.35752	223.1577116	8.9498	0.0132	HOMO->L+10 (29%), HOMO->L+11 (14%), HOMO->L+12 (20%)
30	44895.23918	222.7407668	-3.8698	0.005	H-1->L+3 (64%), H-1->L+4 (10%)
31	44971.86185	222.361263	-10.0062	0.0861	H-6->L+1 (17%), H-2->L+2 (73%)
32	45311.42127	220.6949092	-1.2472	0.1597	H-6->L+1 (36%), H-2->L+2 (10%), H-2->L+3 (35%), H-2->L+4 (12%)
33	45374.33251	220.388917	10.3317	0.0049	H-1->L+4 (68%), H-1->L+5 (16%)
34	45813.90468	218.2743442	-37.5489	0.0425	H-2->L+3 (50%), H-2->L+4 (37%)
35	45916.33709	217.7874071	-2.064	0.0017	H-7->L+1 (93%)
36	45917.9502	217.7797562	13.0268	0.0386	HOMO->L+9 (14%), HOMO->L+10 (23%), HOMO->L+12 (21%), HOMO->L+13 (10%)
37	46006.67118	217.3597816	22.9432	0.0436	HOMO->L+11 (38%), HOMO->L+12 (22%)
38	46507.54149	215.0188911	-36.7343	0.0595	HOMO->L+11 (35%), HOMO->L+13 (18%), HOMO->L+15 (27%)
39	46663.20649	214.301604	-23.6949	0.059	HOMO->L+13 (41%), HOMO->L+14 (26%)
40	46962.43818	212.9361334	43.9209	0.0138	H-2->L+5 (47%), H-2->L+6 (31%)
41	47051.15917	212.534615	-38.0673	0.0417	H-5->L+2 (10%), H-3->L+2 (42%), H-3->L+3 (19%)
42	47389.10548	211.0189652	-0.7714	0.0008	HOMO->L+14 (22%), HOMO->L+15 (46%)
43	47756.8943	209.3938508	-0.0004	0	H-9->LUMO (100%)
44	47931.91661	208.6292539	34.5081	0.0551	H-1->L+9 (10%), HOMO->L+14 (13%), HOMO->L+16 (24%), HOMO->L+19 (19%)
45	48089.19472	207.9469215	-5.5892	0.0026	H-8->L+1 (89%)
46	48106.93892	207.8702205	13.1878	0.0184	H-8->L+1 (10%), H-1->L+6 (17%), HOMO->L+16 (25%)
47	48198.07957	207.4771462	-17.2591	0.0382	H-1->L+6 (20%), H-1->L+8 (13%), HOMO->L+16 (13%)

48	48298.89887	207.0440576	6.1037	0.0047	H-2->L+5 (29%), H-2->L+6 (48%)
49	48319.06273	206.9576568	0.7092	0.0004	H-10->LUMO (84%)
50	48501.34403	206.1798533	-1.1245	0.004	H-1->L+6 (12%), H-1->L+7 (64%)

Table S18. Cartesian coordinates of conformer 2 of **4**

Standard orientation:					
Center Number	**Atomic Number**	**Atomic Type**	**Coordinates (Angstroms)**		
			X	**Y**	**Z**
1	8	0	3.649891	2.803253	-0.358259
2	8	0	2.311719	-0.526962	1.761444
3	8	0	4.581221	1.276068	-2.087431
4	1	0	4.300585	2.125164	-1.620097
5	8	0	4.387938	-3.416184	-1.39092
6	8	0	5.118229	-1.118679	-2.991161
7	1	0	5.264783	-0.208369	-3.308684
8	8	0	-8.982357	-0.41867	0.820386
9	6	0	3.462817	0.471408	-0.070941
10	8	0	-8.181757	-2.312079	-0.085665
11	1	0	-8.921851	-2.640886	0.458332
12	6	0	4.169133	0.265379	-1.291552
13	6	0	3.270947	1.86124	0.374945
14	6	0	4.135798	-2.131353	-1.022737
15	6	0	3.068662	-3.215394	0.997896
16	1	0	3.910749	-3.91504	0.981159
17	1	0	2.223551	-3.747637	0.539426
18	6	0	3.06029	-0.712735	0.629318
19	6	0	3.416998	-1.986363	0.189771
20	6	0	4.485651	-1.0101	-1.775796
21	6	0	2.662828	2.259111	1.707321
22	1	0	3.112384	3.225002	1.959432
23	1	0	2.91443	1.5334	2.48186
24	6	0	-0.189909	-1.513343	0.778694
25	1	0	0.28382	-0.673357	0.272326
26	6	0	-6.134594	-0.625996	-1.45263
27	6	0	1.731719	-1.660545	2.460505
28	6	0	0.410103	-2.067469	1.835511
29	1	0	-0.068142	-2.911827	2.337623
30	6	0	-8.166548	-0.958691	0.090329
31	6	0	1.501185	-1.155305	3.890428
32	1	0	2.454553	-0.890048	4.360639
33	1	0	1.020526	-1.932918	4.494231
34	1	0	0.852025	-0.274221	3.885538
35	6	0	-2.99479	-0.308145	-0.91414
36	1	0	-2.535289	-0.658502	-1.842319
37	6	0	2.727994	-2.830081	2.436459
38	1	0	2.303326	-3.683466	2.978394
39	1	0	3.634988	-2.52073	2.972424
40	6	0	0.614581	3.531388	0.768349
41	6	0	0.108845	3.258367	-0.509975
42	1	0	0.065447	2.228789	-0.859654
43	6	0	1.115211	2.419367	1.666991
44	1	0	0.664414	1.466365	1.375432
45	1	0	0.793016	2.614122	2.69833

46	6	0	-1.509509	-1.965457	0.1955
47	1	0	-1.861477	-2.852297	0.742829
48	1	0	-1.347448	-2.274196	-0.846492
49	6	0	-7.132805	-0.208347	-0.640279
50	1	0	-7.233643	0.858233	-0.452924
51	6	0	-2.583095	-0.883769	0.229768
52	6	0	0.64838	4.867095	1.19694
53	1	0	1.031274	5.101068	2.189042
54	6	0	-4.005044	0.792302	-1.102378
55	1	0	-3.499465	1.653029	-1.565352
56	1	0	-4.398011	1.145542	-0.14427
57	6	0	-5.20157	0.426687	-2.027833
58	1	0	-5.764543	1.347801	-2.21978
59	1	0	-4.811244	0.082494	-2.994975
60	6	0	-0.296141	5.613646	-0.903774
61	1	0	-0.64541	6.416194	-1.548549
62	6	0	-0.340549	4.288059	-1.341757
63	1	0	-0.722978	4.053366	-2.332383
64	6	0	0.199404	5.900144	0.372036
65	1	0	0.234854	6.928011	0.725049
66	6	0	-3.100624	-0.548622	1.607564
67	1	0	-3.880286	0.215972	1.601523
68	1	0	-2.286723	-0.197551	2.255237
69	1	0	-3.516841	-1.445988	2.087202
70	6	0	5.545127	-3.748655	-2.175866
71	1	0	6.434062	-3.240248	-1.788554
72	1	0	5.402163	-3.486727	-3.22529
73	1	0	5.657503	-4.829335	-2.064905
74	6	0	-5.835367	-2.043084	-1.859343
75	1	0	-6.46398	-2.779112	-1.362721
76	1	0	-4.780923	-2.268488	-1.65581
77	1	0	-5.970031	-2.14203	-2.946341

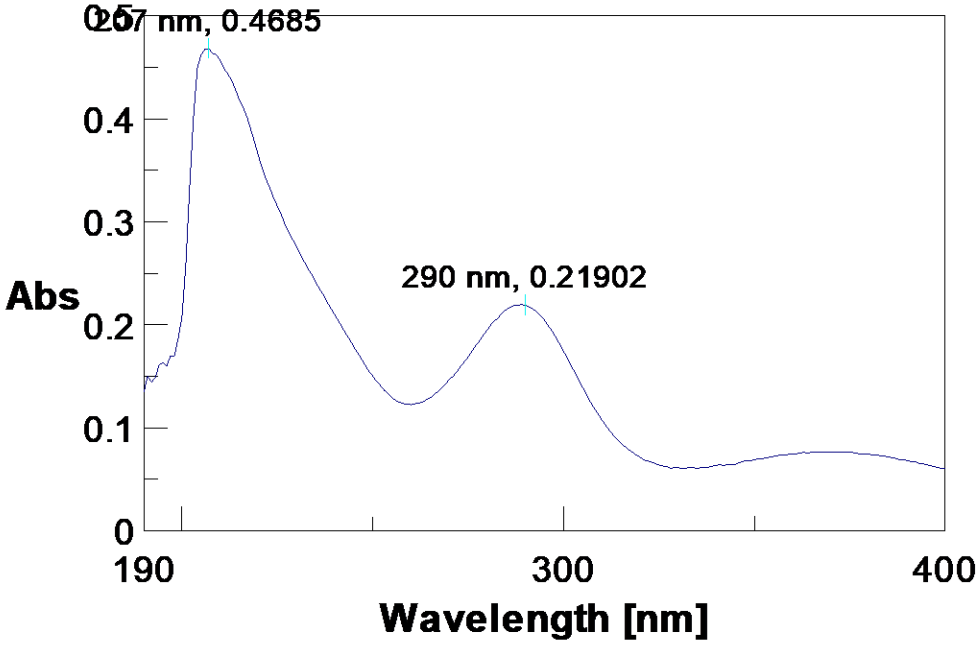

Fig. S9. UV spectrum of **1** in MeOH

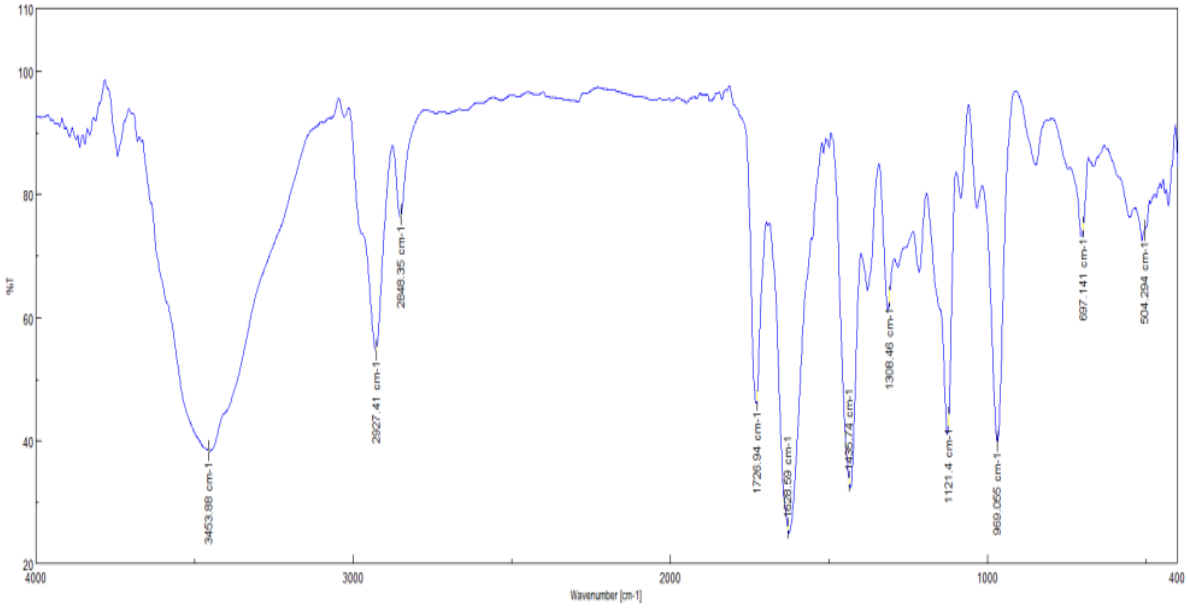

Fig. S10. IR spectrum of **1** (KBr disc)

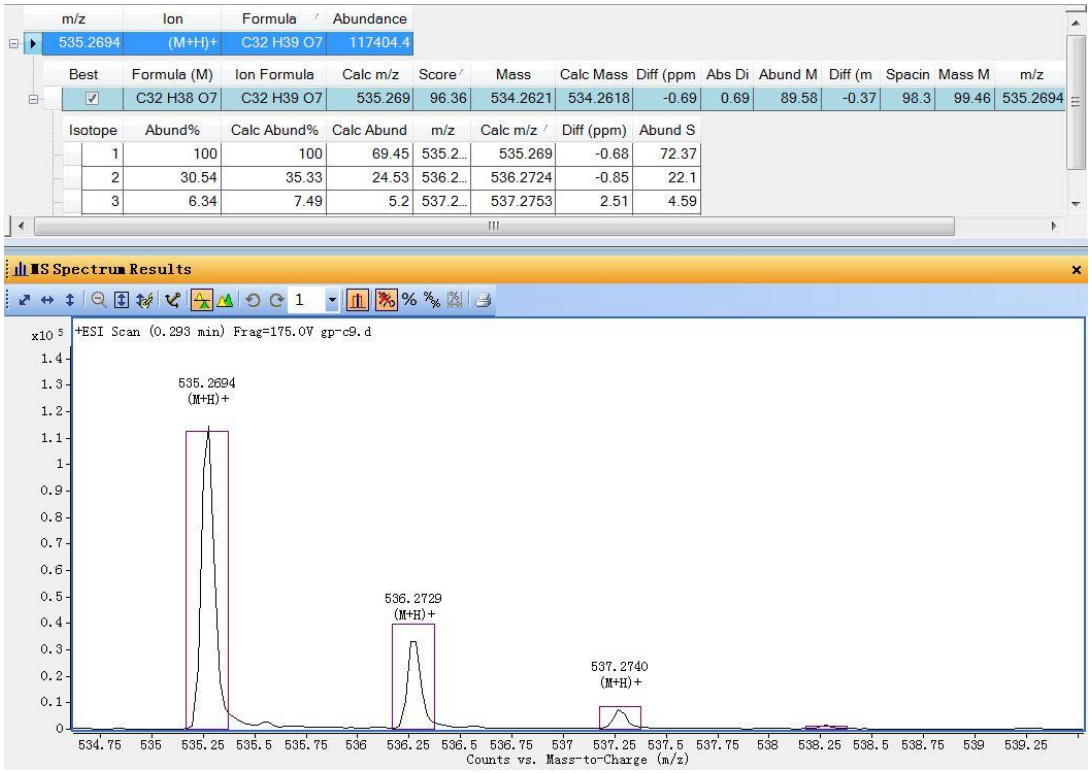

Fig. S11. HR-ESI-MS spectrum of **1**

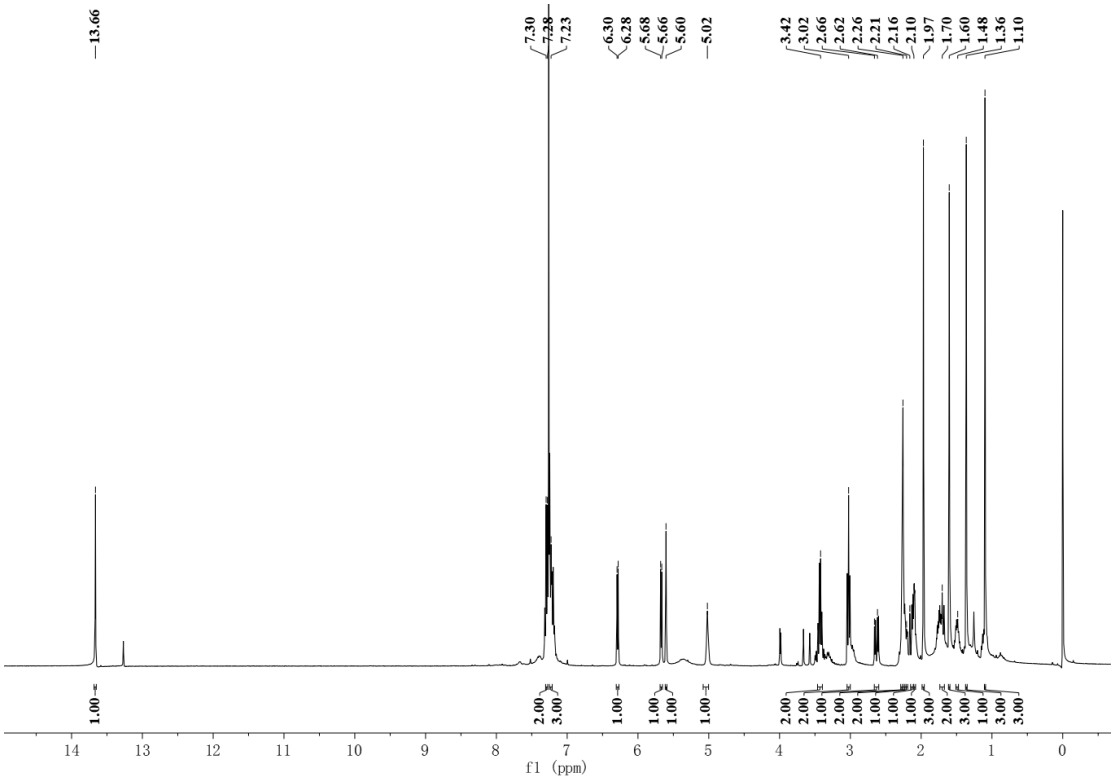

Fig. S12. ^{1}H NMR spectrum of **1** in $CDCl_3$

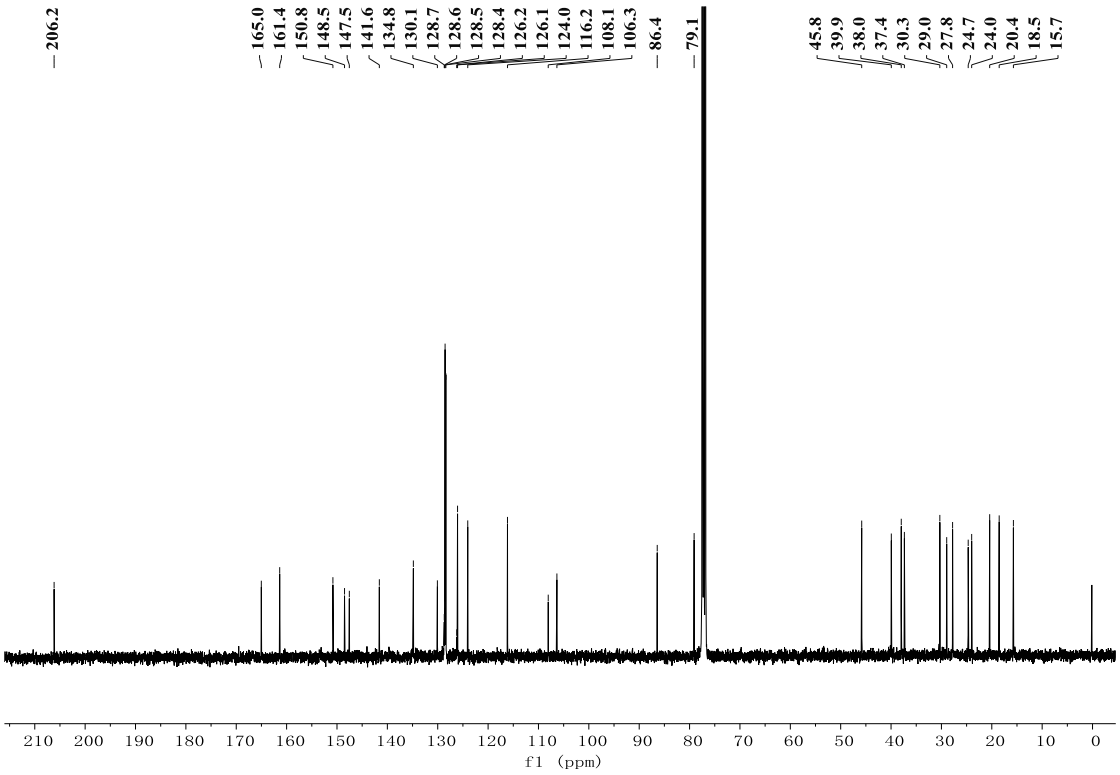

Fig. S13. ^{13}C NMR spectrum of **1** in $CDCl_3$

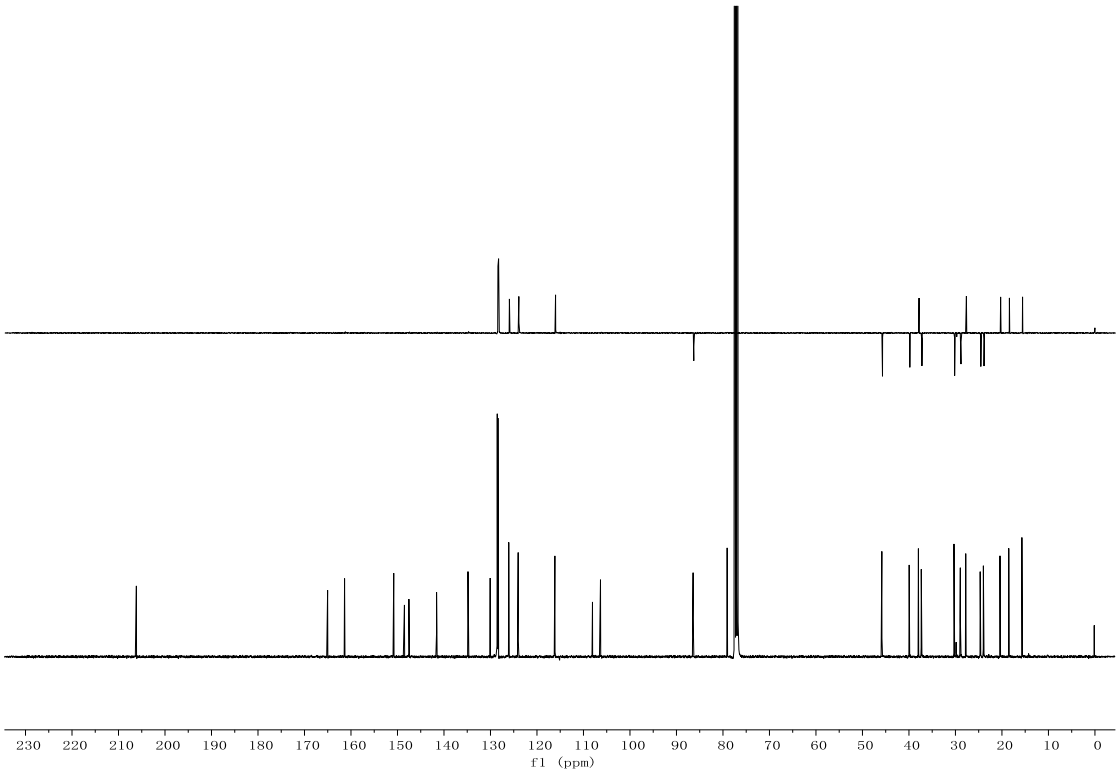

Fig. S14. DEPT-135 and ^{13}C NMR spectra of **1** in $CDCl_3$

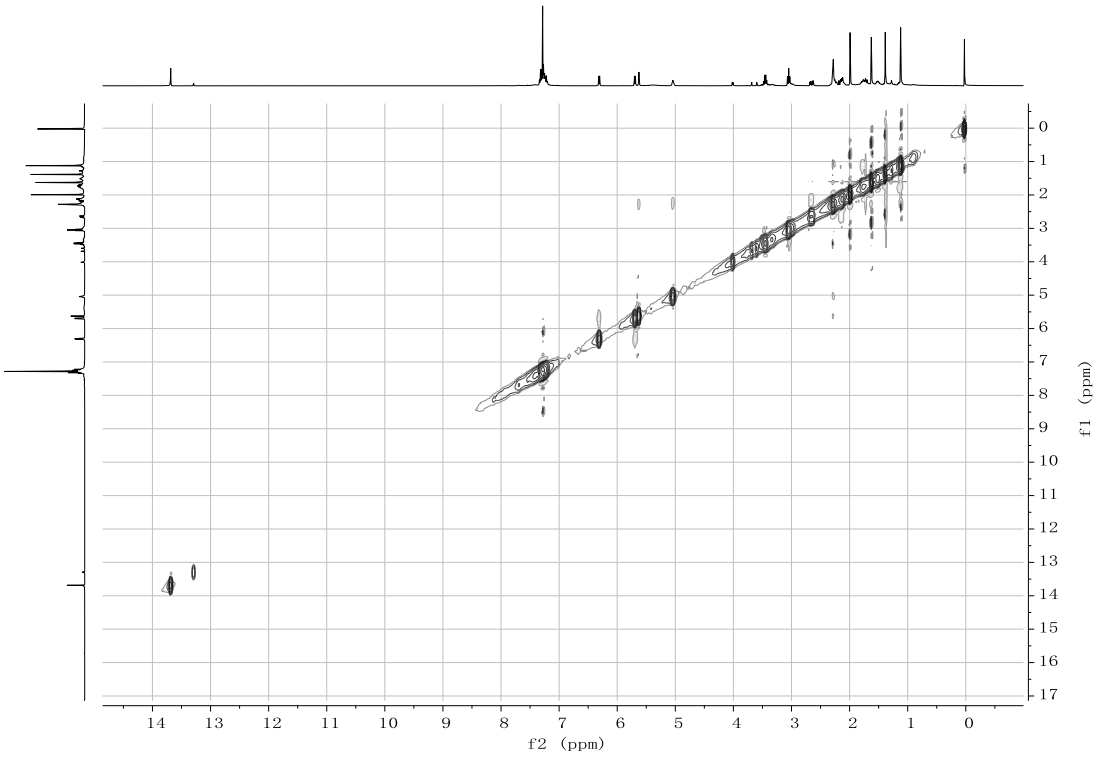

Fig. S15. ^{1}H-^{1}H COSY spectrum of **1** in $CDCl_3$

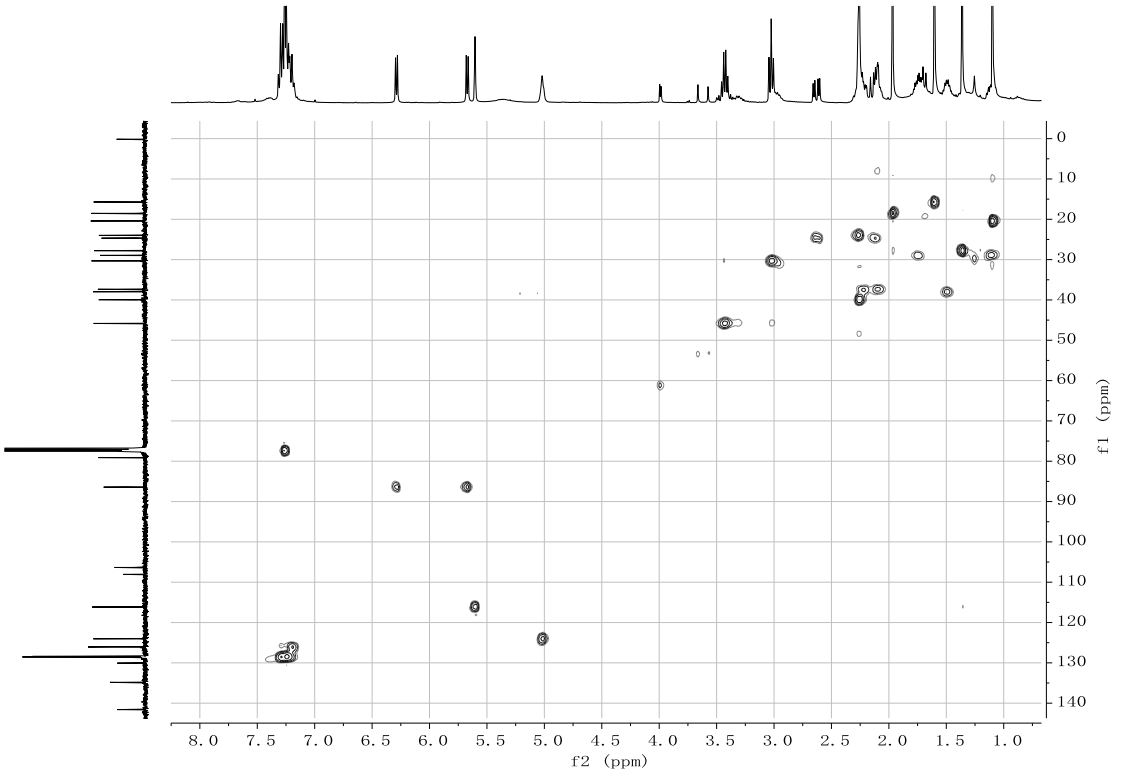

Fig. S16. HSQC spectrum of **1** in $CDCl_3$

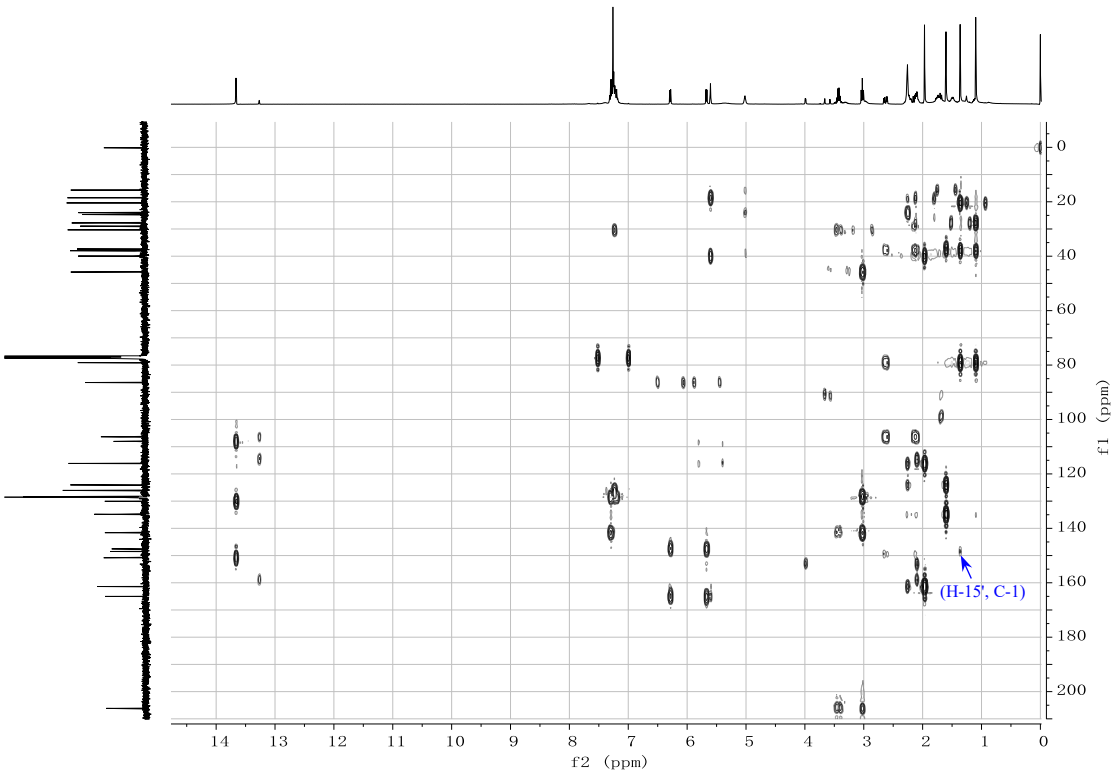

Fig. S17. HMBC spectrum of **1** in $CDCl_3$

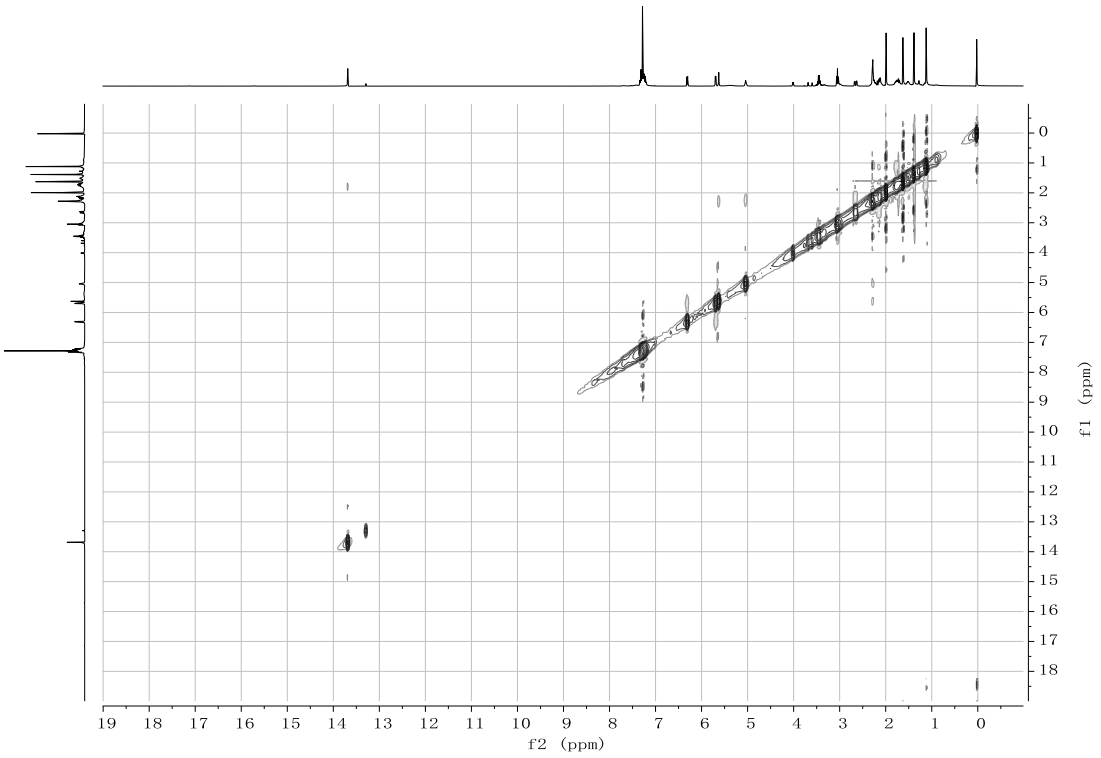

Fig. S18. NOESY spectrum of **1** in $CDCl_3$

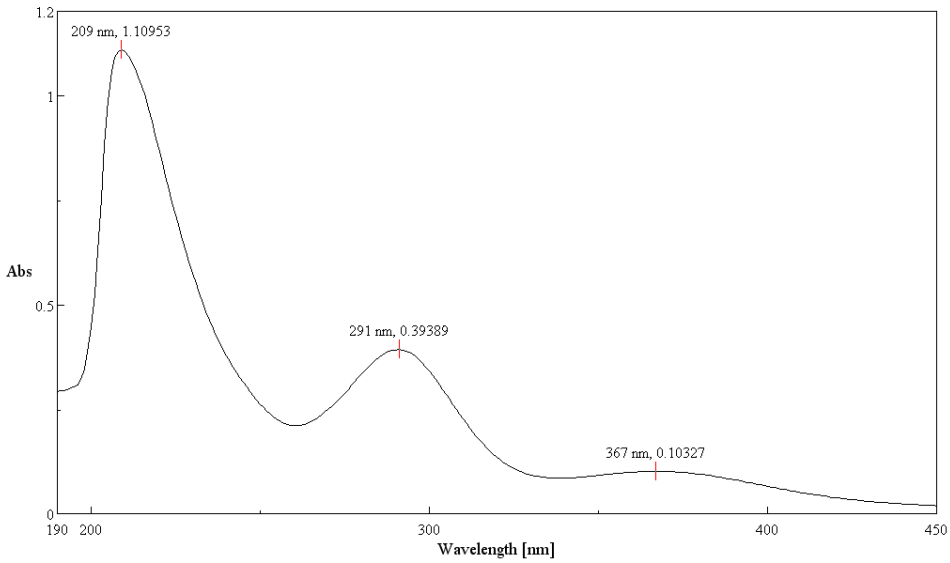

Fig. S19. UV spectrum of **2** in MeOH

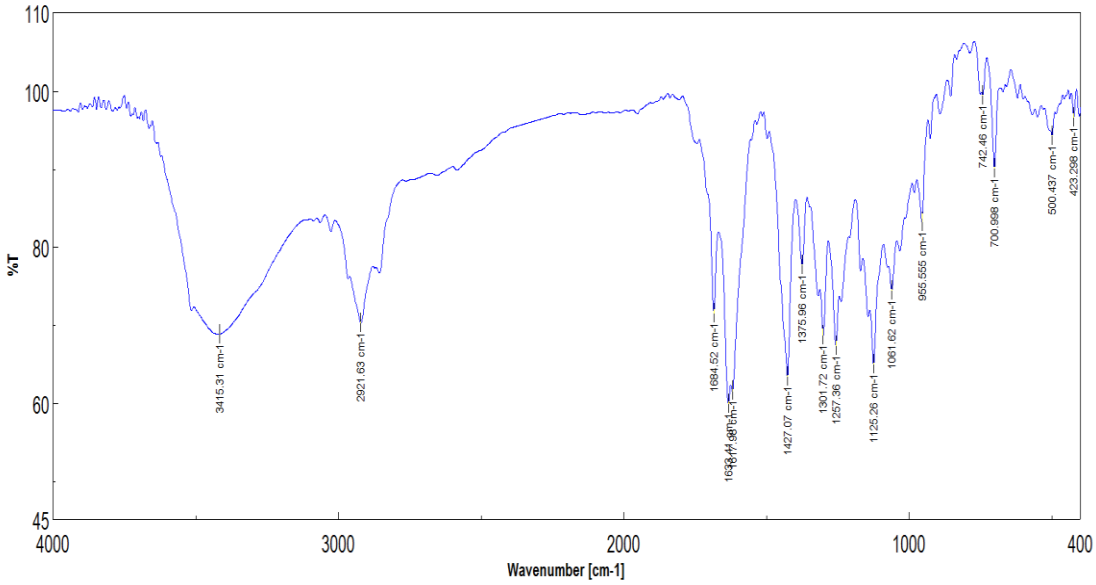

Fig. S20. IR spectrum of **2** (KBr disc)

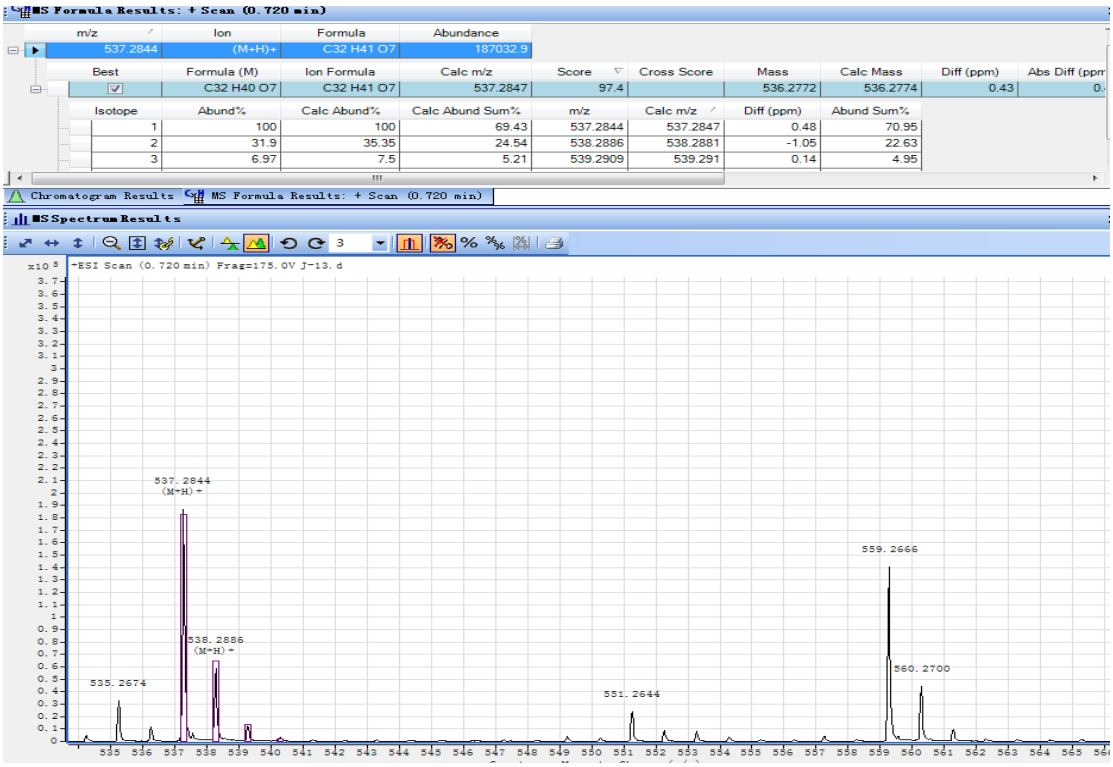

Fig. S21. HR-ESI-MS spectrum of **2**

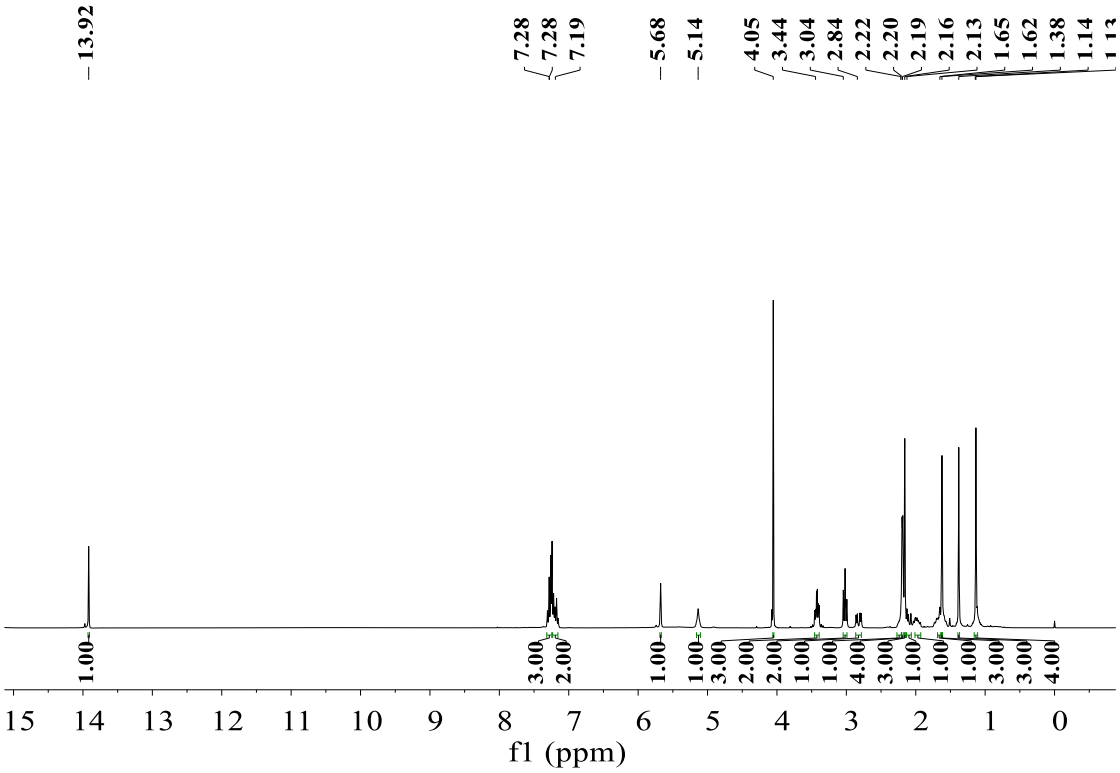

Fig. S22. ^{1}H NMR spectrum of **2** in $CDCl_3$

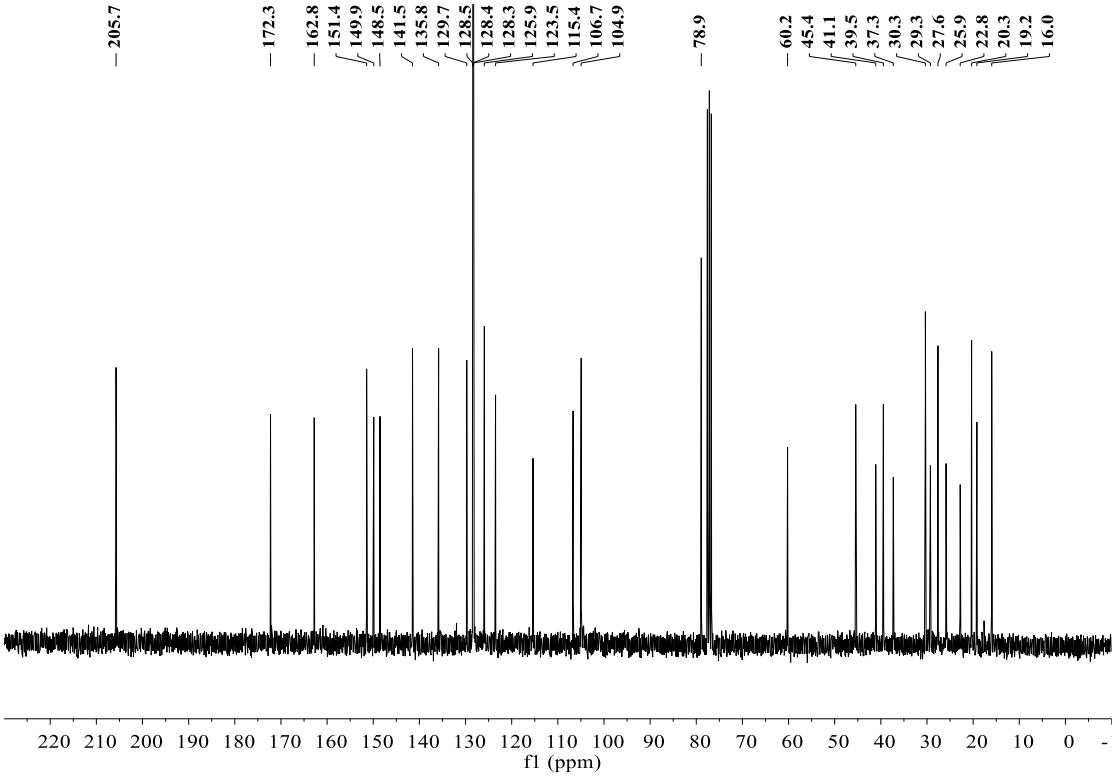

Fig. S23. ^{13}C NMR spectrum of **2** in $CDCl_3$

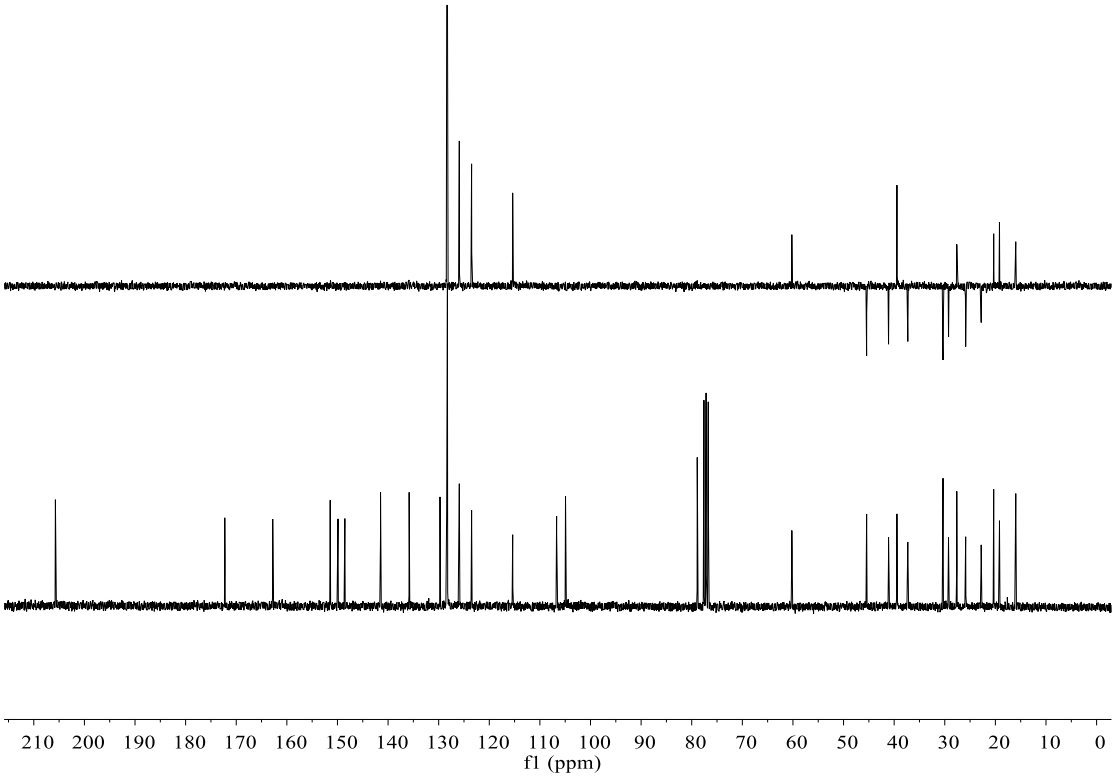

Fig. S24. DEPT-135 and ^{13}C NMR spectra of **2** in $CDCl_3$

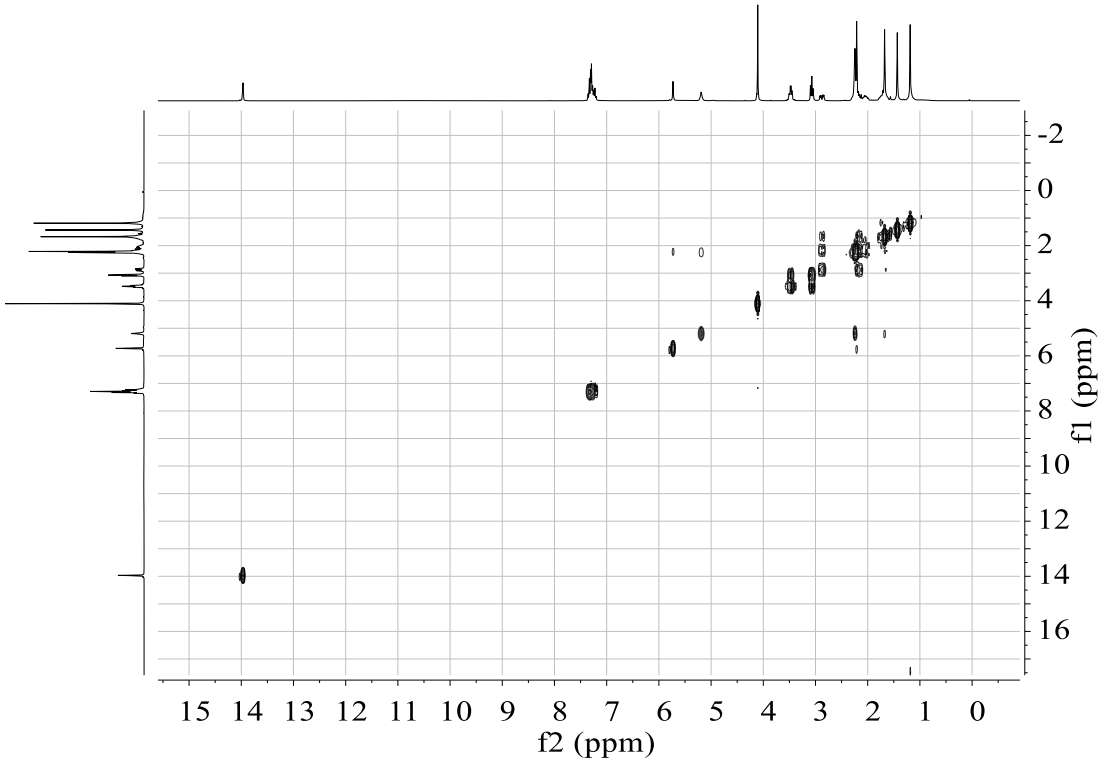

Fig. S25. ^{1}H-^{1}H COSY spectrum of **2** in $CDCl_3$

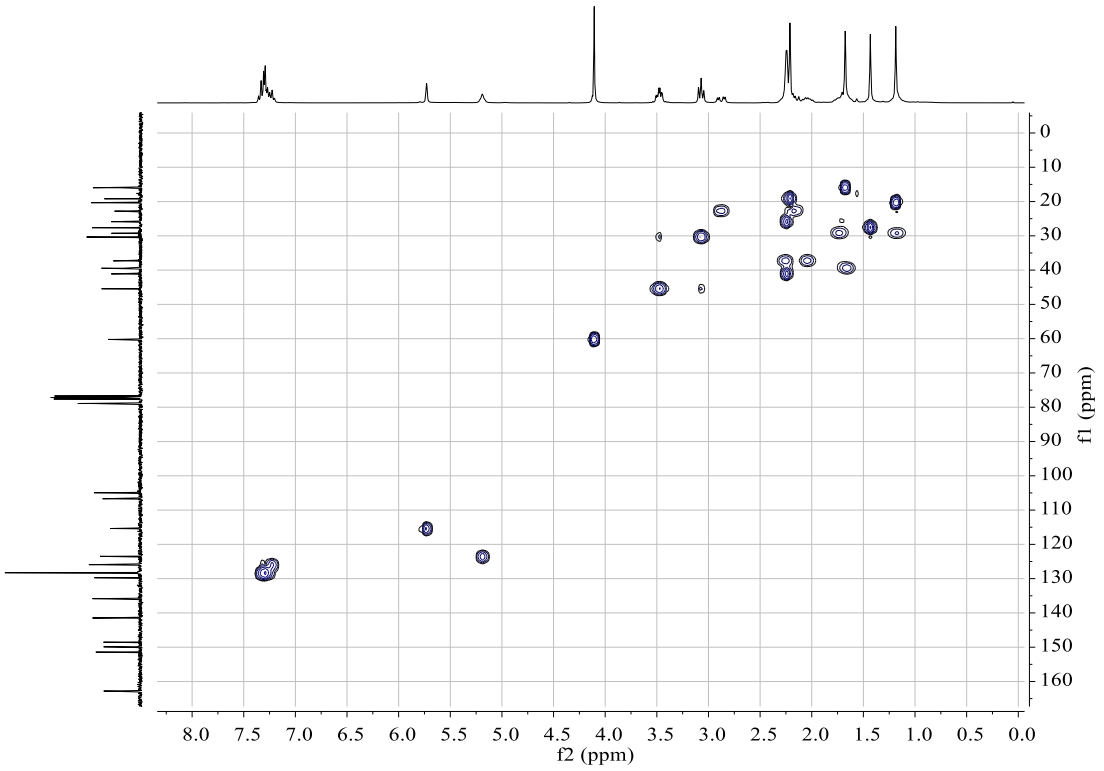

Fig. S26. HSQC spectrum of **2** in $CDCl_3$

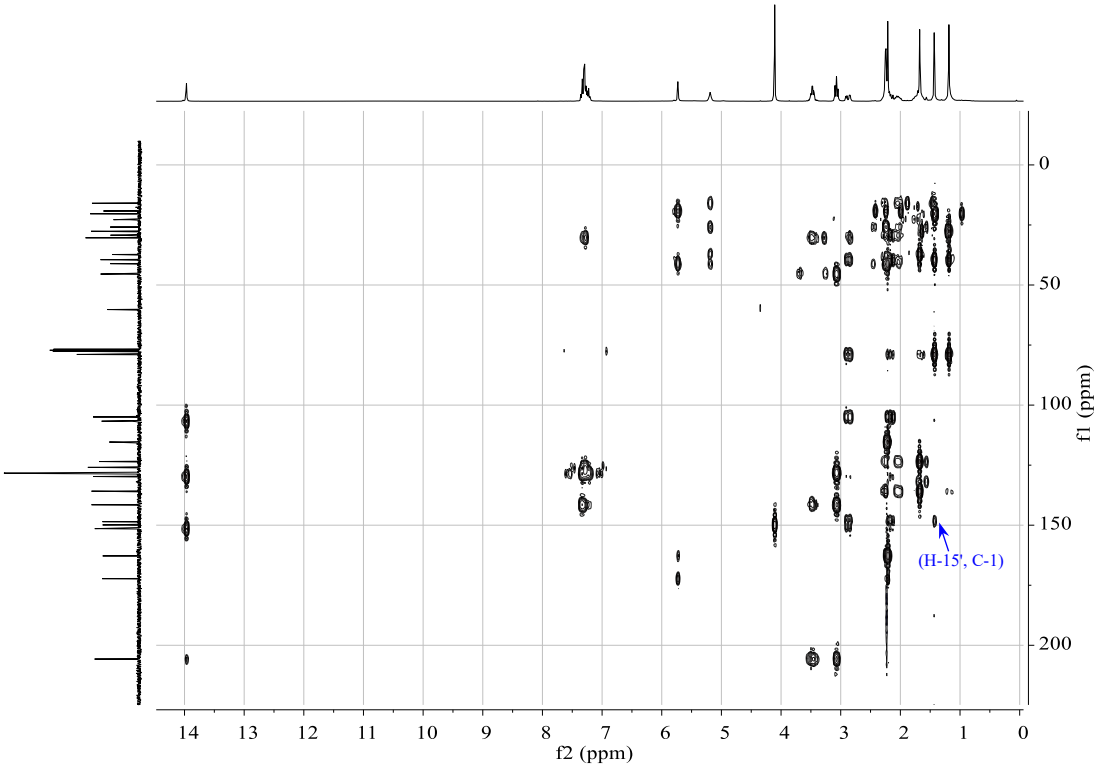

Fig. S27. HMBC spectrum of **2** in $CDCl_3$

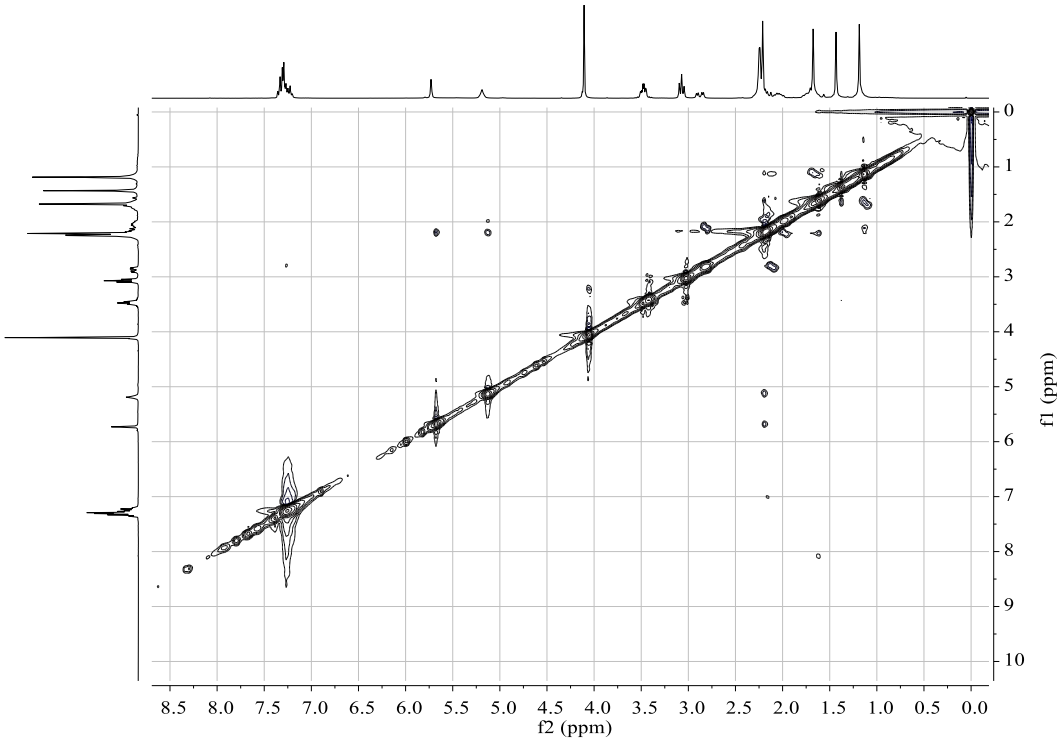

Fig. S28. NOESY spectrum of **2** in $CDCl_3$

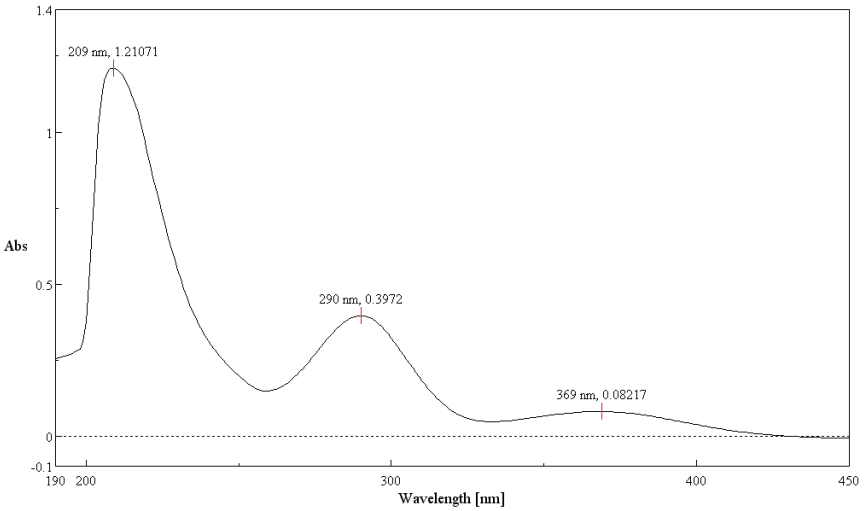

Fig. S29. UV spectrum of **3** in MeOH

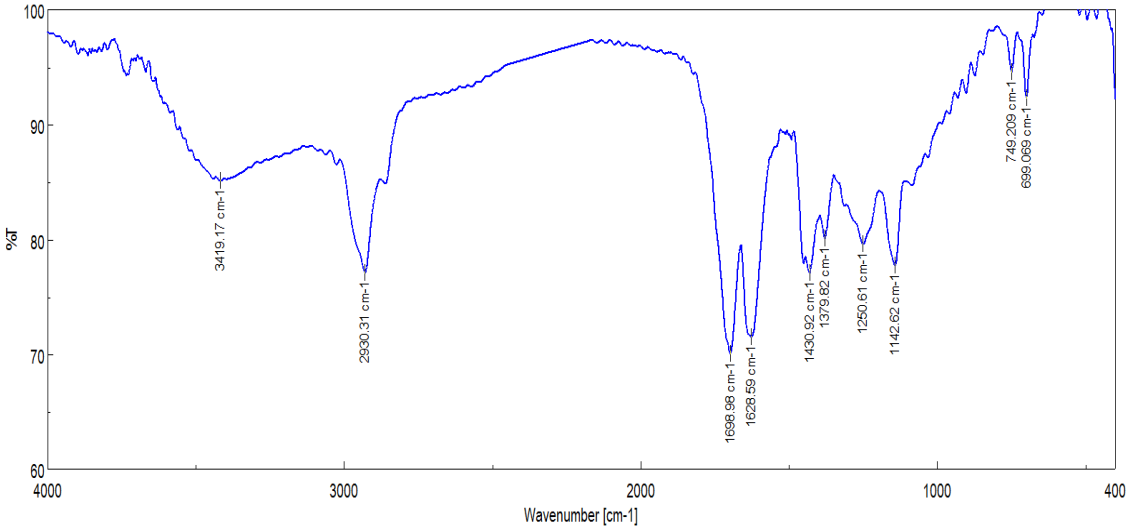

Fig. S30. IR spectrum of **3** (KBr disc)

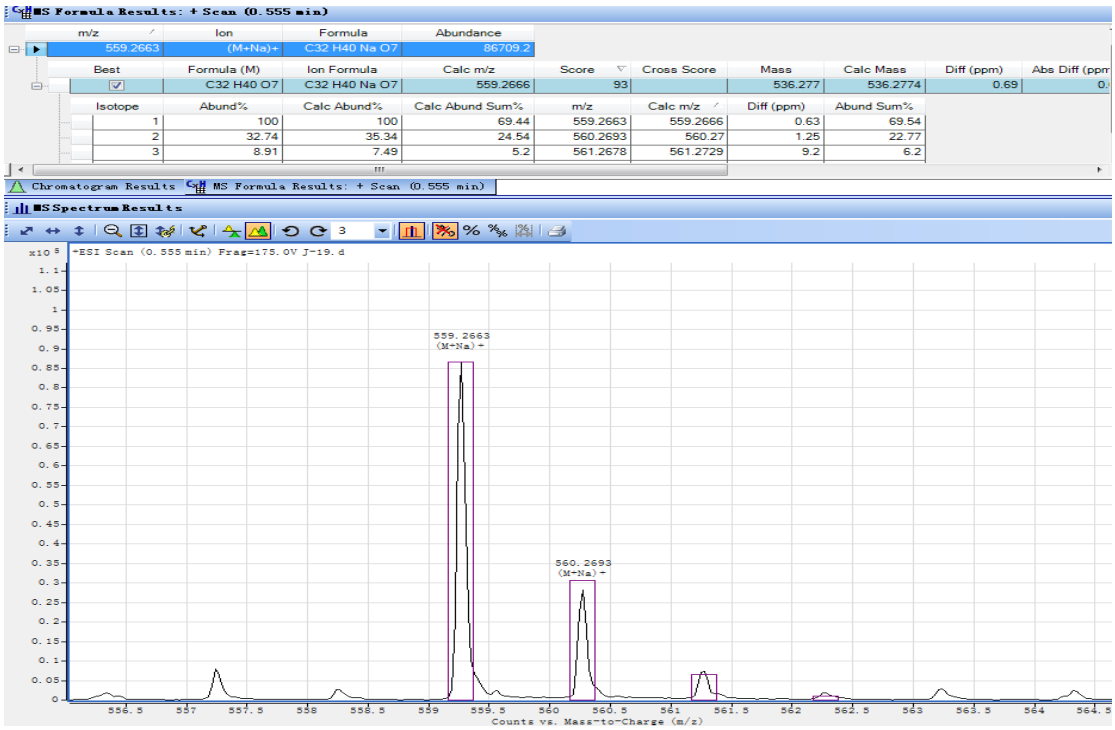

Fig. S31. HR-ESI-MS spectrum of **3**

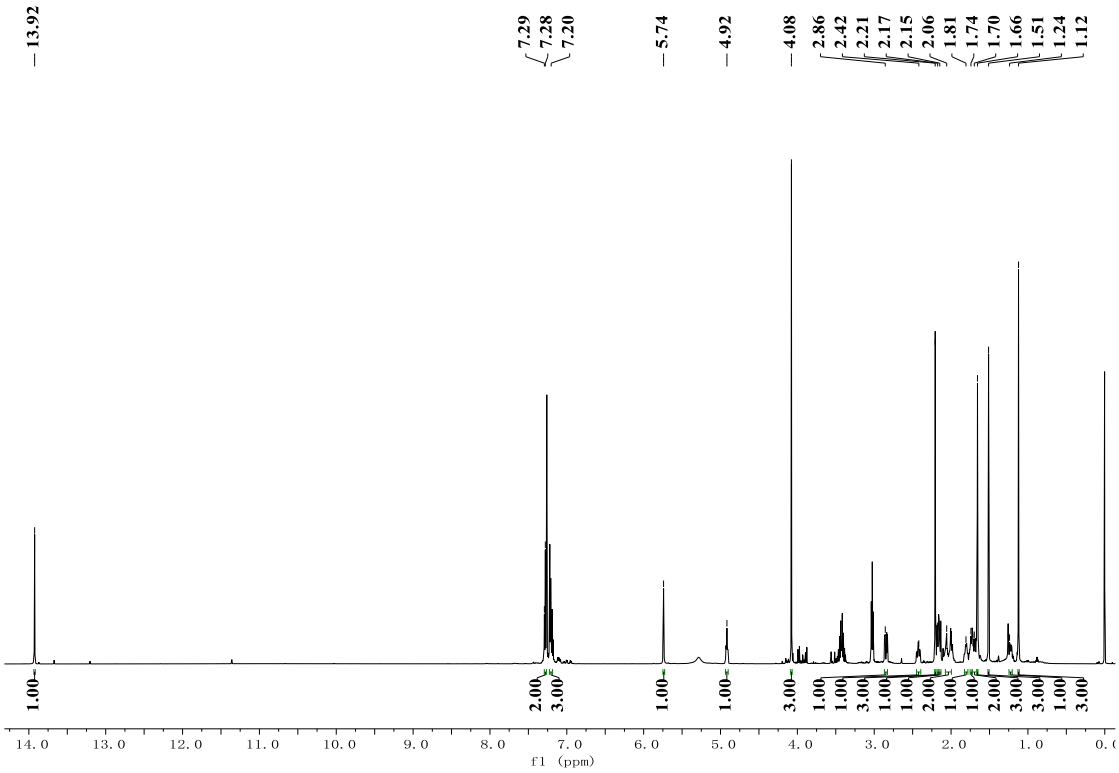

Fig. S32. ^{1}H NMR spectrum of **3** in $CDCl_3$

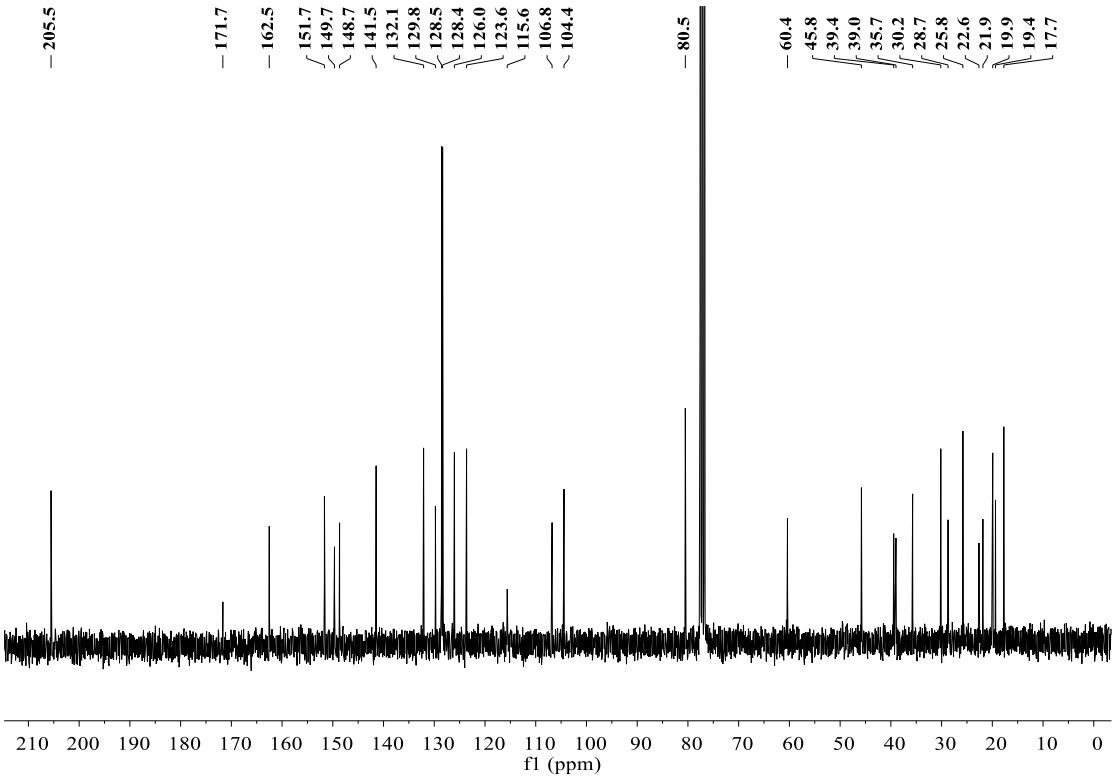

Fig. S33. ^{13}C NMR spectrum of **3** in $CDCl_3$

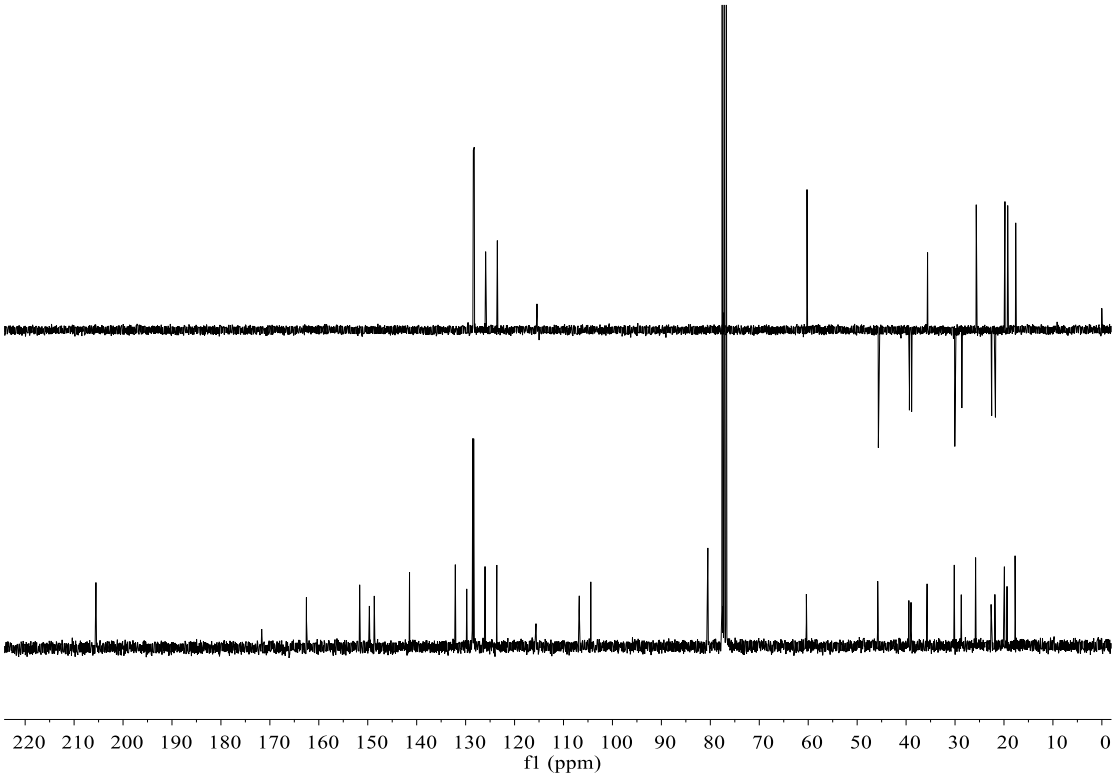

Fig. S34. DEPT-135 and ^{13}C NMR spectra of **3** in $CDCl_3$

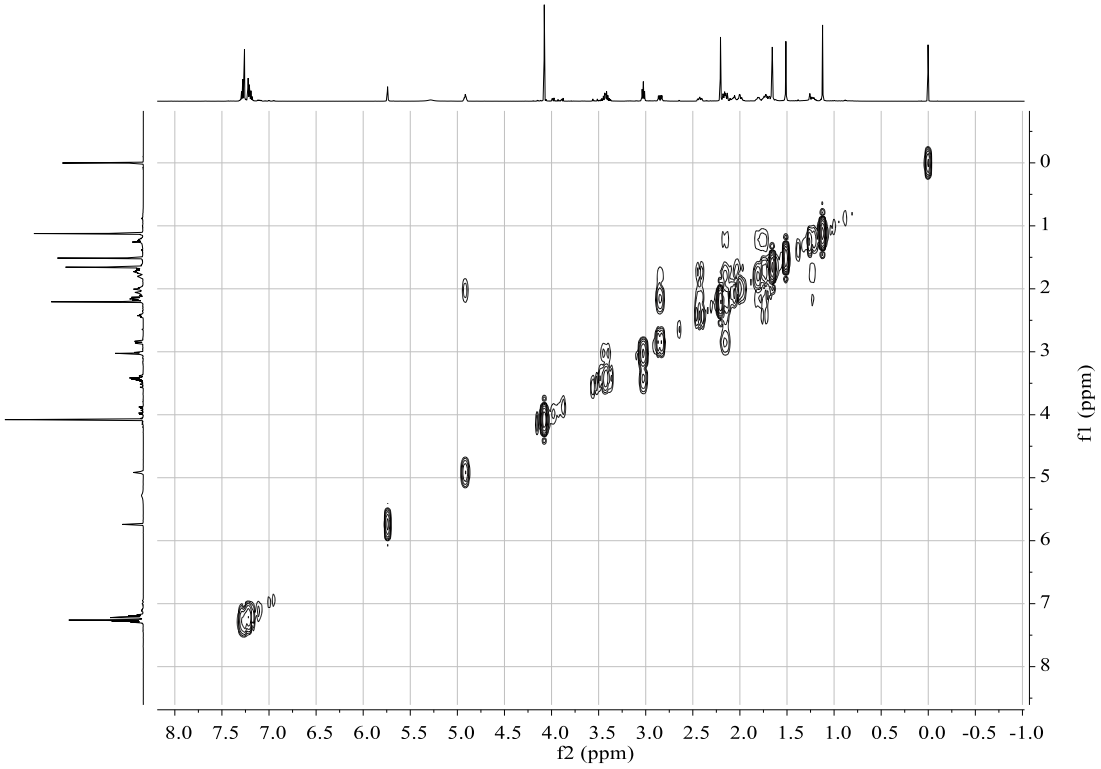

Fig. S35. ^{1}H-^{1}H COSY spectrum of **3** in $CDCl_3$

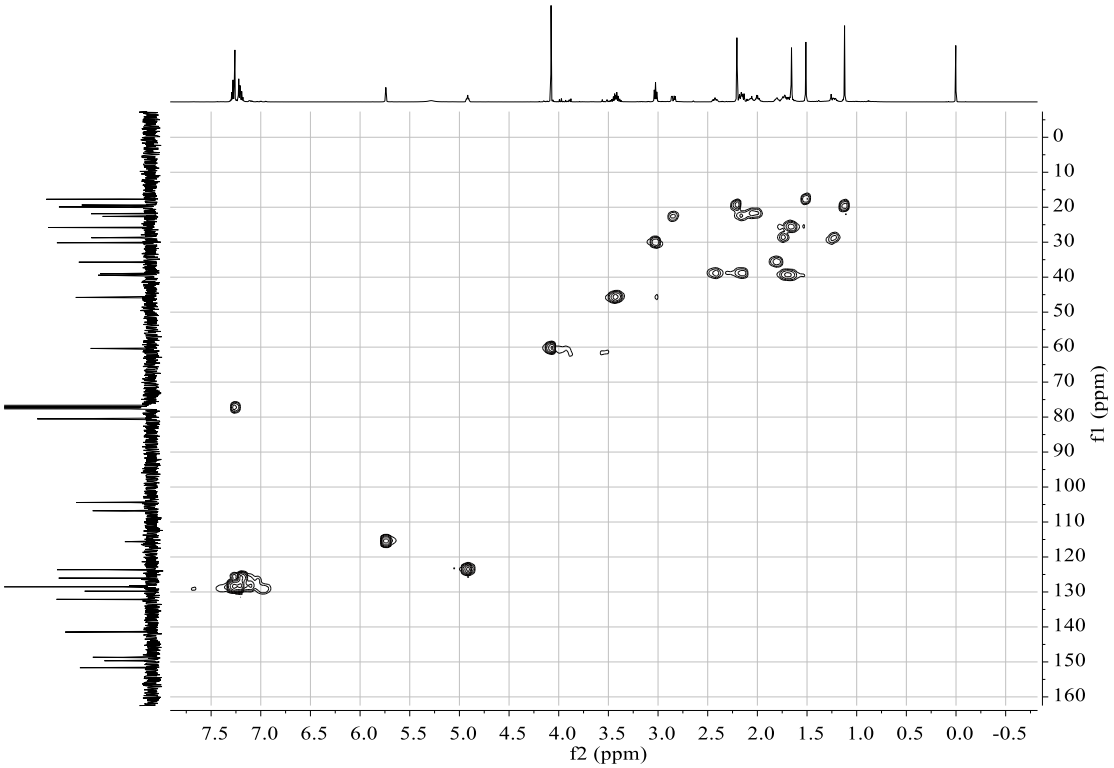

Fig. S36. HSQC spectrum of **3** in $CDCl_3$

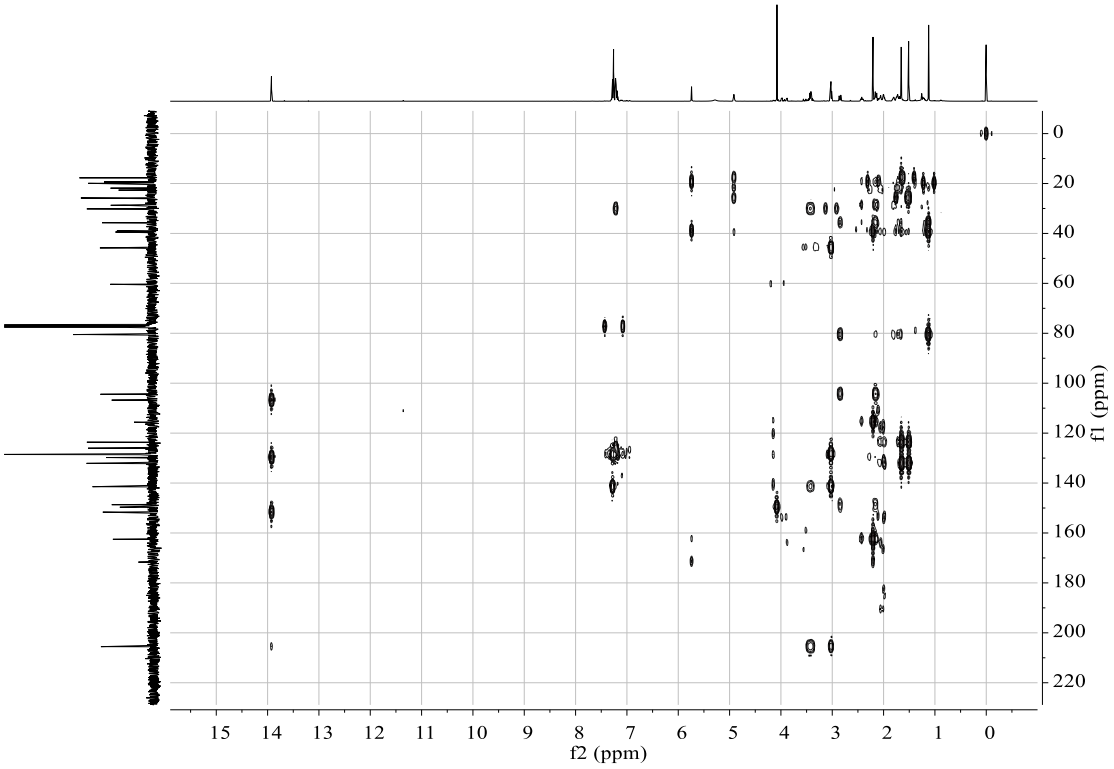

Fig. S37. HMBC spectrum of **3** in $CDCl_3$

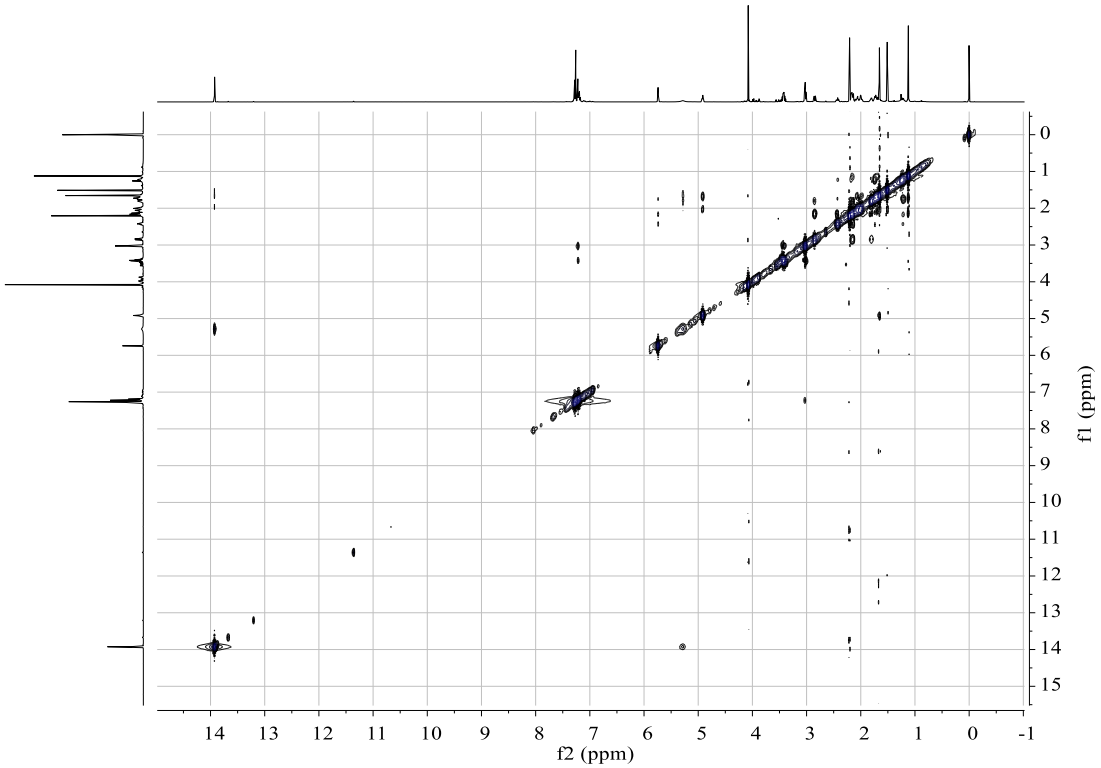

Fig. S38. NOESY spectrum of **3** in $CDCl_3$

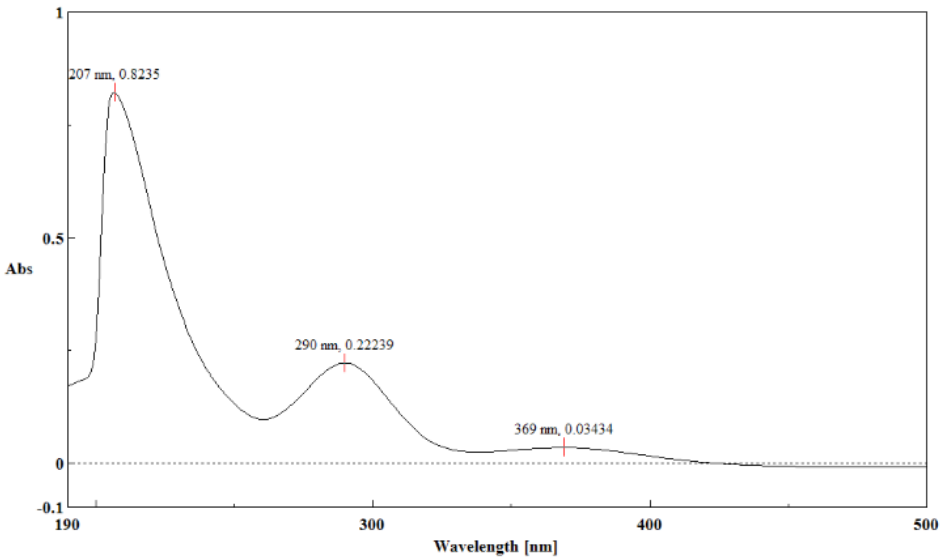

Fig. S39. UV spectrum of **4** in MeOH

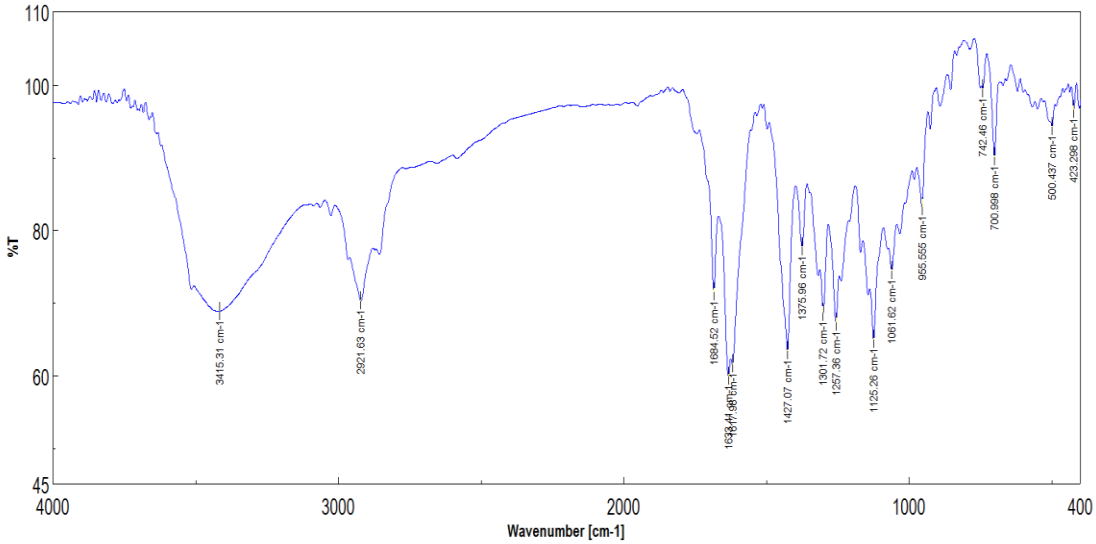

Fig. S40. IR spectrum of **4** (KBr disc)

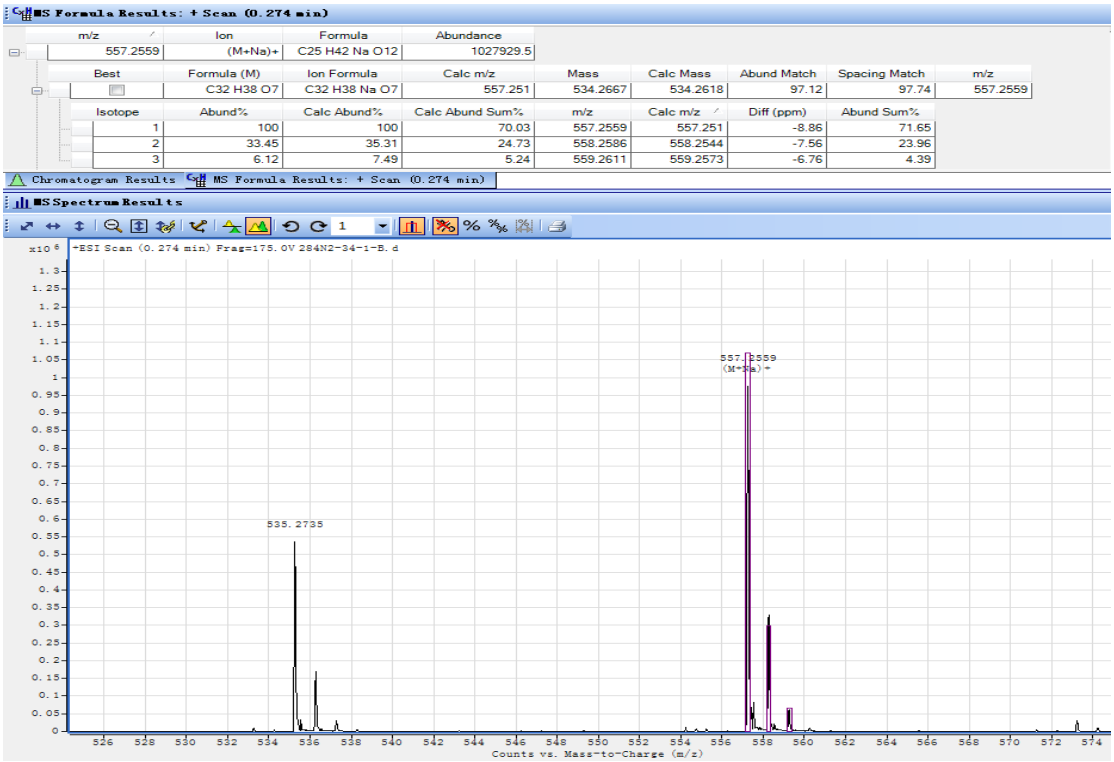

Fig. S41. HR-ESI-MS spectrum of **4**

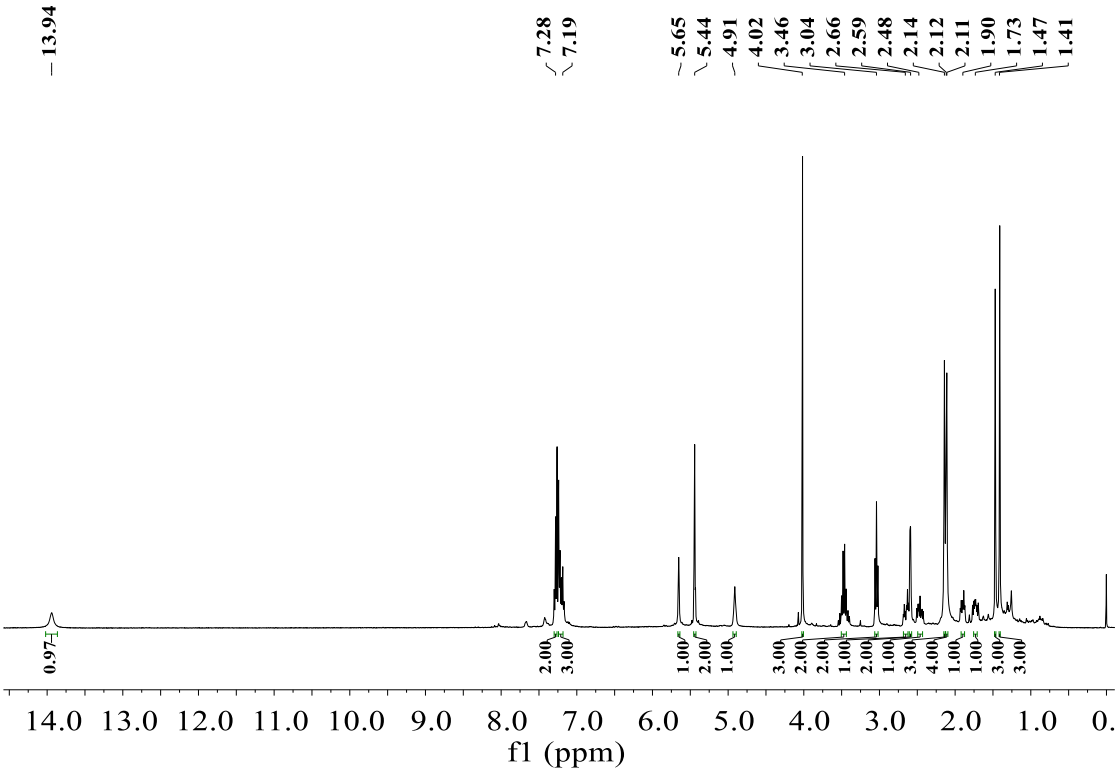

Fig. S42. ^{1}H NMR spectrum of **4** in $CDCl_3$

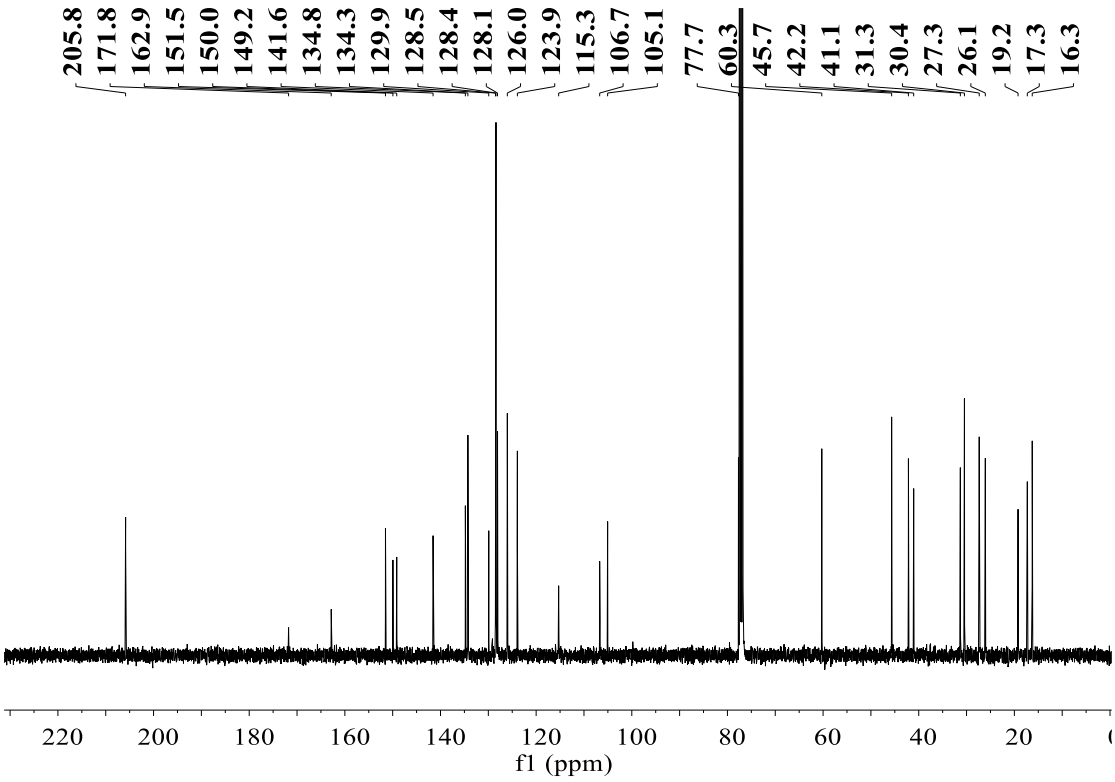

Fig. S43. ^{13}C NMR spectrum of **4** in $CDCl_3$

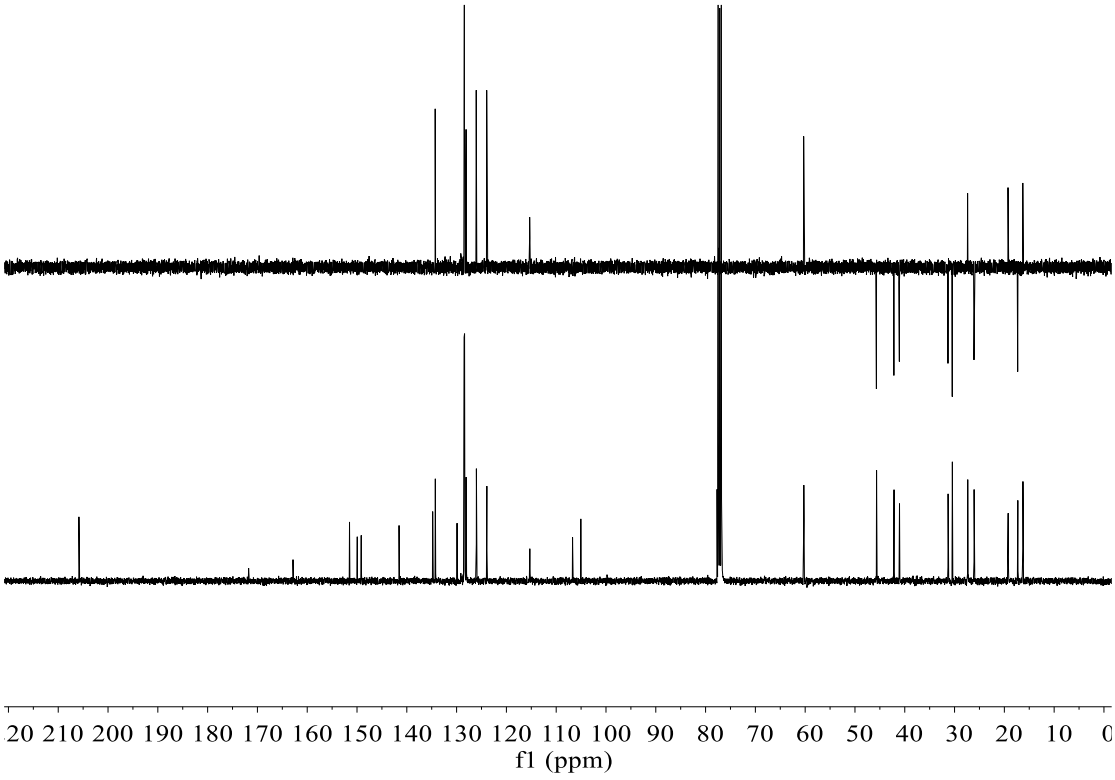

Fig. S44. DEPT-135 and ^{13}C NMR spectra of **4** in $CDCl_3$

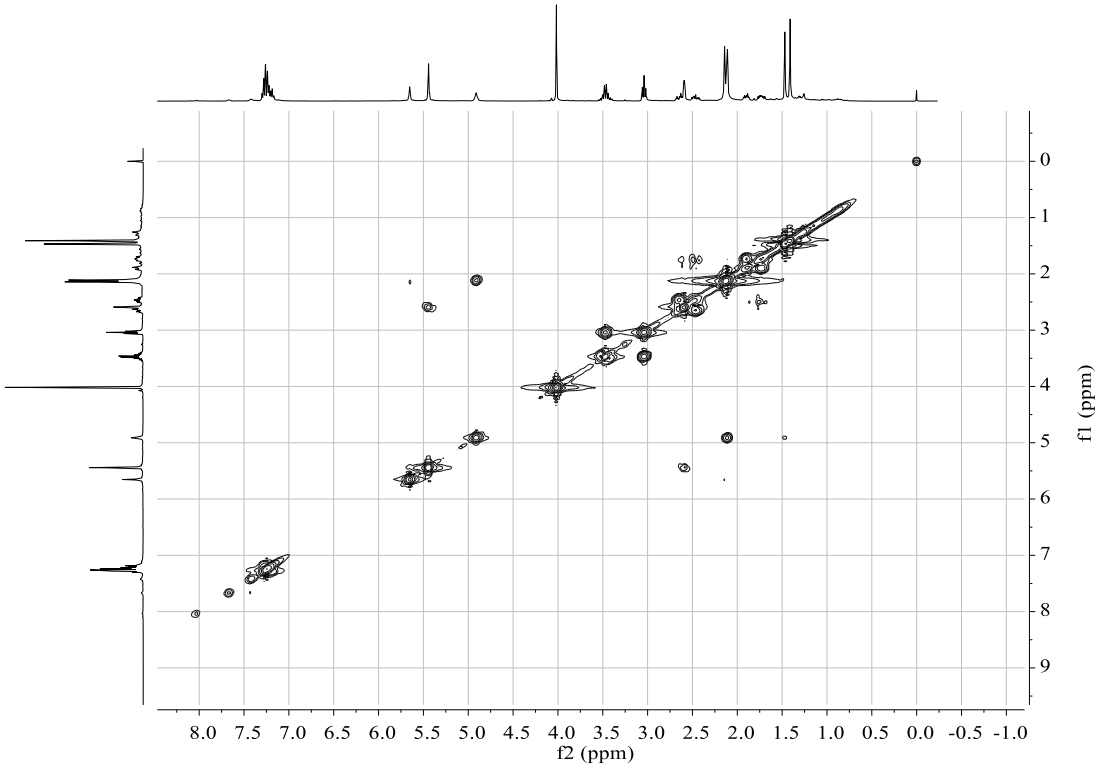

Fig. S45. ^{1}H-^{1}H COSY spectrum of **4** in $CDCl_3$

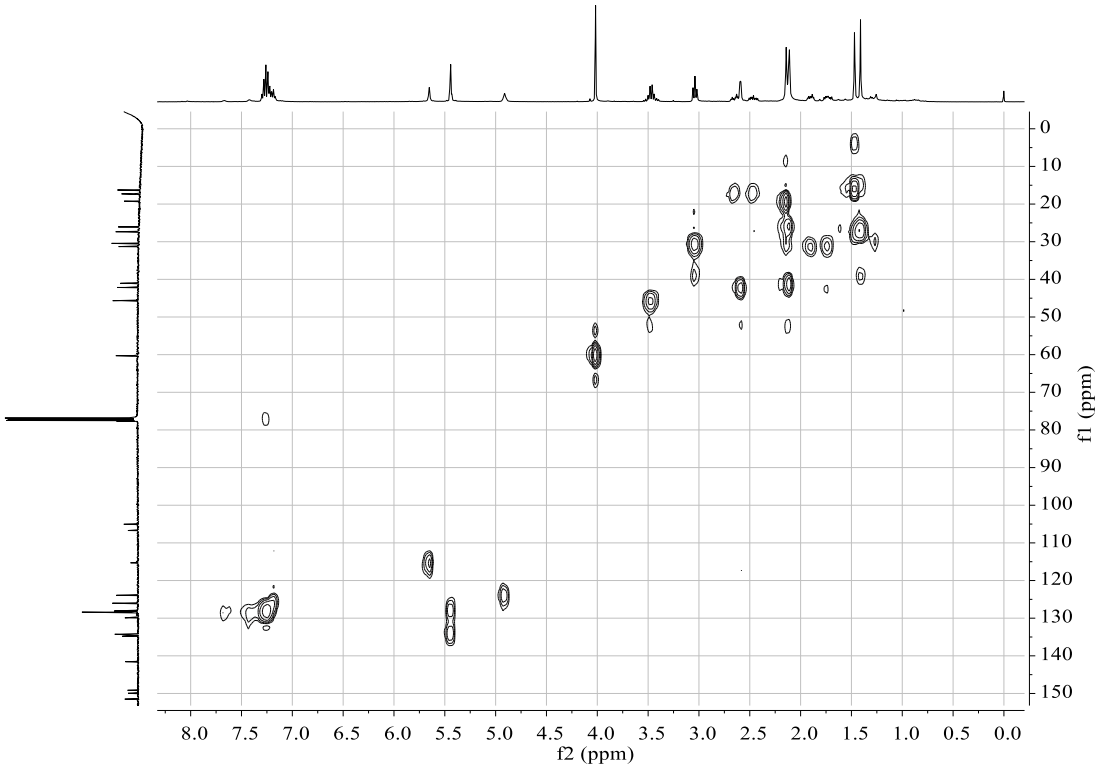

Fig. S46. HSQC spectrum of **4** in $CDCl_3$

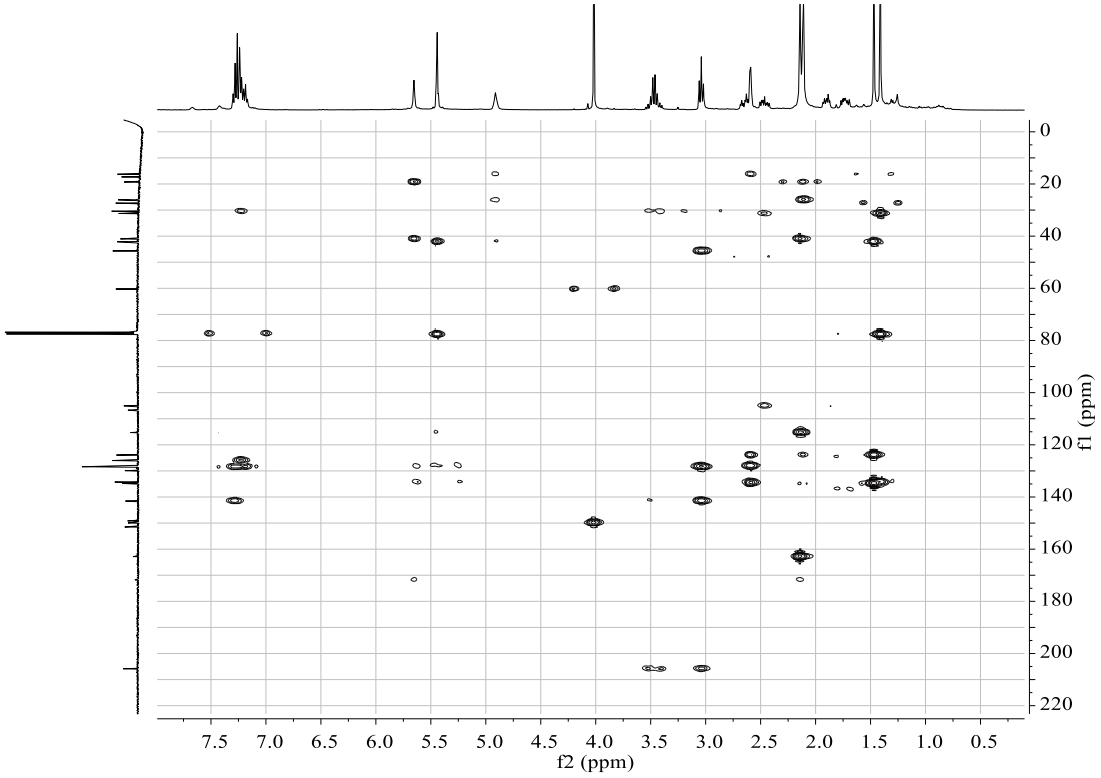

Fig. S47. HMBC spectrum of **4** in $CDCl_3$

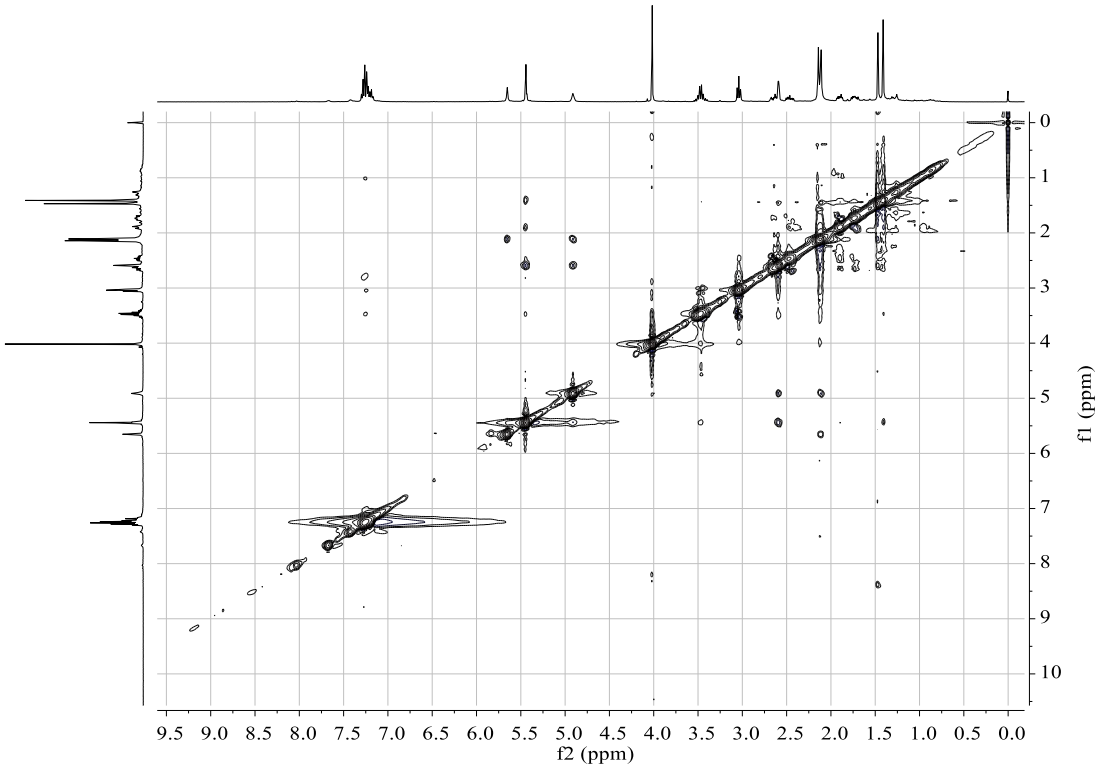

Fig. S48. NOESY spectrum of **4** in $CDCl_3$

Reference

[1]. X. L. Zhang, Y. P. Xia, P. B. Li, Z. N. Wu, R. L. Li, J. L. Cai, Y. B. Zhang, G. C. Wang, Y. L. Li, W. Tang, W. W. Su. Discovery of cyperenoic acid as a potent and novel entry inhibitor of influenza A virus, *Antiviral Research*, **2024**, 105822.

[2]. W. Tang, Y. Y. Li, Q. Y. Song, Z. Q. Wang, M. M. Li, Q. W. Zhang, Y. Wang, W. C. Ye, Y. L. Li. Mechanism of cross-resistance to fusion inhibitors conferred by the K394R mutation in respiratory syncytial virus fusion protein. *Journal of Virology*, **2021**, 95(20), e01205-21.

[3]. Gaussian 09, Revision A.02, M. J. Frisch, G. W. Trucks, H. B. Schlegel, G. E. Scuseria, M. A. Robb, J. R. Cheeseman, G. Scalmani, V. Barone, B. Mennucci, G. A. Petersson, H. Nakatsuji, M. Caricato, X. Li, H. P. Hratchian, A. F. Izmaylov, J. Bloino, G. Zheng, J. L. Sonnenberg, M. Hada, M. Ehara, K. Toyota, R. Fukuda, J. Hasegawa, M. Ishida, T. Nakajima, Y. Honda, O. Kitao, H. Nakai, T. Vreven, J. A. Montgomery, Jr., J. E. Peralta, F. Ogliaro, M. Bearpark, J. J. Heyd, E. Brothers, K. N. Kudin, V. N. Staroverov, R. Kobayashi, J. Normand, K. Raghavachari, A. Rendell, J. C. Burant, S. S. Iyengar, J. Tomasi, M. Cossi, N. Rega, J. M. Millam, M. Klene, J. E. Knox, J. B. Cross, V. Bakken, C. Adamo, J. Jaramillo, R. Gomperts, R. E. Stratmann, O. Yazyev, A. J. Austin, R. Cammi, C. Pomelli, J. W. Ochterski, R. L. Martin, K. Morokuma, V. G. Zakrzewski, G. A. Voth, P. Salvador, J. J. Dannenberg, S. Dapprich, A. D. Daniels, O. Farkas, J. B. Foresman, J. V. Ortiz, J. Cioslowski, and D. J. Fox, Gaussian, Inc., Wallingford CT, **2009**.

[4]. T. Bruhn, A. Schaumloffel, Y. Hemberger, G. Pescitelli, SpecDis version 1.71, Berlin, Germany, **2017**, http://specdis-software.jimdo.com